UNIVERSITY OF THE AEGEAN – SCHOOL OF ENVIROMENT– DEPARTMENT OF MARINE SCIENCES

ESTIMATION OF VERTICAL MIXING IN THE NORTH AEGEAN SEA BASED ON ARGO FLOAT DATA

Naomi Krauzig

BACHELOR'S THESIS

Supervisor: Prof. Vassilis Zervakis

Mytilene, September 2016

BACHELOR'S THESIS

Graduate of the Department of Marine Sciences

Naomi Krauzig

THESIS TOPIC:

Estimations of Vertical Mixing in the North Aegean Sea based on Argo float data

Examination Committee		Signatures
Advisor:	**Prof. Vassilis Zervakis**	
First Examiner:	**Prof. Elina Tragou**	
Second Examiner:	**Prof. Evangelia Krasakopoulou**	

Acknowledgements

I would like to express my gratitude to all those who gave me the possibility to complete this thesis. Especially, I want to thank Prof. Vassilis Zervakis for his excellent supervision during my thesis and the interesting topic he provided for me. Furthermore, I would like to thank him for his patient guidance during my whole undergraduate study period and during the Erasmus Placement exchange. Without his continuous help, the significant amount of specialized lectures, workshops, exercises, and field studies, I would not have been able to approach a project with such interest and specialty.

Also, I want to thank Prof. Evangelia Krasakopoulou and Prof. Elina Tragou for their significant support and advices, especially during the Erasmus Placement period, despite their busy schedule.

I'd also like to thank all the professors at the University of the Aegean for their guidance and motivation throughout the past 4 years. Due to their patience and openness I got the opportunity to learn and experience, using practically knowledge and developing sets of skills through the elaboration on particular research projects.

Of course, I thank my mother for being a dedicated reader, for her infectious curiosity and all her support throughout the years. And finally, I must thank my closest friends and fellow students who have helped me, taught me, and enriched my experience for their unending generosity.

Abstract

The North Aegean Sea is considered as a region of deep water formation in the Mediterranean. Dense water formation events are known to take place rather infrequently and in the time intervals between such events, the bottom waters are excluded from interaction with other water masses through advection. In order to examine the evolution of deep waters during those periods at shorter-than-annual time scales, new, high-frequency data from a profiling ARGO float were analyzed. The specific MedArgo float (nr.6901884) was trapped during 2014-2015 within the deep Athos basin, and remained there for 13 months. The analyzed hydrographic profiles point out that the Black Sea Water surface layer is an effective isolator between the deep layers of the North Aegean and the atmosphere, absorbing large amounts of heat and buoyancy as well as hindering dense water formation. Also, the temporal evolution of the averaged potential density anomaly possibly reveals short-termed dense-water formation that affected layers shallower than 600 m and was followed (after March 2015) by a longer-termed stagnation period lasting till November 2015. It seems that the water masses deeper than 600m remain almost constant, without being affected by the dominant seasonal cycle. It could be possible to conclude, that the replenishment of deep basins takes place in longer-than-annual cycles, since the seasonal cycle seems to affect only the upper water masses. It is noteworthy, that the vertical eddy diffusion coefficient K_S (based on the observed rate of change of salinity) indicated a positive conductivity sensor drift of the profiling float. Furthermore, the conductivity corrections verified a remarkable drift in salinity of 0,0039 to 0,0112 psu during the stagnation period due to the increasing conductivity sensor drift rate of $4{,}6748\times10^{-5}$ mmho day^{-1}. After correcting the sensor's drift, the eddy diffusion coefficients $K_{\sigma\theta}$, K_S, K_T were found to range between $6\text{-}7\times10^{-5}$ and $2\text{-}3\times10^{-3}$ m^2s^{-1} for the deeper than 400m waters. Considering that the deep basins of the North Aegean are practically isolated below the 400m threshold during the stagnation period, the good agreement of the three diffusion coefficients K_c and the fact that the properties of deeper water masses slide along the θ-S curve towards lower densities suggests that the dominant process in vertical diffusion is turbulent mixing.

Περίληψη

Το Βόρειο Αιγαίο θεωρείται μια από τις περιοχές δημιουργίας βαθέων υδάτων της Μεσογείου. Τα επεισόδια σχηματισμού πυκνού νερού είναι σχετικά σποραδικά και κατά τις ενδιάμεσες περιόδους στασιμότητας, τα βαθιά στρώματα είναι πλήρως απομονωμένα από οριζόντιες μεταφορές. Προκειμένου να μελετηθεί η εξέλιξη των βαθέων υδάτων σε υποετήσιες χρονικές κλίμακες, αναλύθηκαν νέα δεδομένα υψηλής συχνότητας ενός πλωτήρα ARGO. Ο συγκεκριμένος πλωτήρας MedArgo (υπ'αριθμόν 6901884) εγκλωβίστηκε το 2014 στη βαθιά λεκάνη του Άθω για 13 μήνες. Η ανάλυση των υδρογραφικών δεδομένων υποδηλώνει ότι το επιφανειακό στρώμα της Μαύρης Θάλασσας λειτουργεί σαν μονωτής θερμοκρασίας και πλευστότητας μεταξύ υδάτινων στρωμάτων και ατμόσφαιρας, παρεμποδίζοντας την δημιουργία βαθέων νερών. Παράλληλα, η καταγραφείσα χρονική εξέλιξη της χωρικά ολοκληρωμένης δυναμικής ανωμαλίας πυκνότητας (σ_θ) καταδεικνύει ένα επεισόδιο βραχείας δημιουργίας πυκνών νερών που επηρέασε τα μικρότερα των 600 μέτρων βάθη, το οποίο ακολουθήθηκε, μετά το Μάρτιο 2015, από μια πολύμηνη περίοδο στασιμότητας που κράτησε έως το Νοέμβριο 2015. Θα μπορούσε να συναχθεί το συμπέρασμα ότι ανανέωση των βαθέων λεκανών λαμβάνει χώρα σε υπερετήσιους κύκλους, καθώς οι βαθιές μάζες νερού (>600m) φαίνεται να μη επηρεάζονται από τον κυρίαρχο εποχικό κύκλο. Είναι αξιοσημείωτο, ότι η εξέλιξη του κατακόρυφου συντελεστή διάχυσης K_S (βασισμένος στον ρυθμό μεταβολής της αλατότητας) φανέρωσε την ολίσθηση του αισθητήρα αγωγιμότητας (sensor drift) του συγκεκριμένου πλωτήρα MedArgo. Επιπλέον, οι διορθώσεις της αγωγιμότητας επιβεβαίωσαν την ύπαρξη ολίσθησης της αλατότητας από 0,0039 έως 0,0112 psu κατά την περίοδο στασιμότητας λόγω του ρυθμού αύξησης της αγωγιμότητας από $4{,}6748\times10^{-5}$ mmho day^{-1}. Μετά από την απαραίτητη διόρθωση εκτιμήθηκε ότι οι κατακόρυφοι συντελεστές διάχυσης $K_{\sigma\theta}$, K_S, K_T κυμαίνονται μεταξύ $6\text{-}7\times10^{-5}$ και $2\text{-}3\times10^{-3}$ m^2s^{-1}. Συμπεραίνοντας, φαίνεται ότι η καλή συμφωνία των τριών συντελεστών διάχυσης K_c καθώς και το γεγονός ότι οι ιδιότητες των βαθέων υδάτινων μαζών κινούνται κατά μήκος της καμπύλης θ-S, προσδιορίζουν ως κυρίαρχη διεργασία κατακόρυφης διάχυσης την τυρβώδους ανάμειξη.

Contents

Acknowledgements 3
Abstract 4
Περίληψη 5
Contents 6
1.) Introduction 7
1.1.) The Study Area 7
1.2.) General surface water characteristics 7
1.3.) Current circulation pattern 8
1.4.) Deep-water formation and stagnation periods 9
2.) Data and Methods 10
2.1.) MedArgo profiling float data 10
2.1.1.) Quality control 11
2.2.) NCEP/NCAR Air-Sea flux data 11
2.3.) EMODNet bathymetry data 11
2.4.) Estimation of the stratification frequency 11
2.5.) Estimation of the eddy diffusion coefficient 12
3.) Results 13
3.1.) Hydrographic characteristics 13
3.1.1.) Vertical variability 15
3.1.2.) Seasonal variability 16
3.2.) Heat Flux 17
3.3.) Mixed layer depth 19
3.4.) Vertical stability 20
3.5.) Vertical diffusion 21
3.4.1.) Corrected vertical diffusion 27
4.) Conclusion and Discussion 30
5.) References 30
Appendix 34
Matlab commands 34

1.) Introduction

1.1.) The Study Area

The North Aegean Sea is a part of the Aegean Sea (Figure 1.) experiencing complex bathymetric and hydrographic conditions (Lykousis et al., 2002). The bottom topography is characterized by a deep trough, separated by shallow sills and shelves, constituting the 'North Aegean Trough' (Poulos et al., 1997). The North Aegean Trough follows a northeast to southwest direction, beginning north of the island of Lemnos and ending at the Sporades island complex.

It is the deepest trench of the North Aegean and includes two deep basins:

i) the Lemnos basin with a maximum depth of 1469 m

ii) the Athos–Sporades basin with a maximum depth of 1476 m

These two basins are isolated below the depth of 550 m. The North Aegean Trough itself is isolated below 350m from the rest of the Aegean and has a water volume of 32×10^{11} m^3, according to Velaoras et al. (2005).

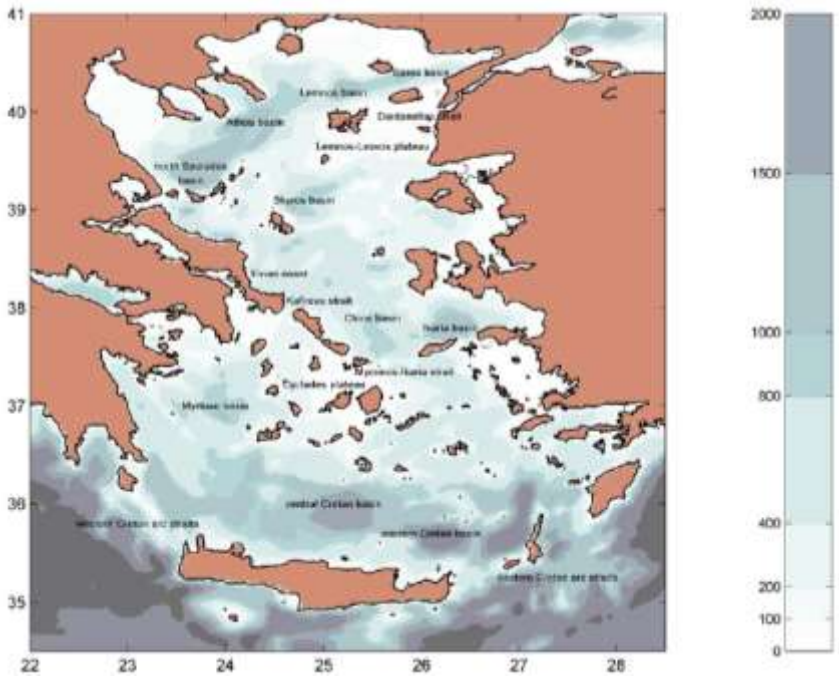

Figure 1.) Aegean bathymetry and major features (Vervatis et al., 2011)

1.2.) General surface water characteristics

Aegean surface temperatures vary from less than 13 °C in winter to more than 24 °C in summer, and salinities from less than 31 to more than 39 (Poulos et al., 1997). As a result of Black Sea outflow, salinity minima of about 26 may locally occur during the summer. As the Levantine Intermediate Water (LIW) travels northward along the Turkish coast, prevailing offshore winds cause upwelling to the surface (Yüce, 1995). In shallow eastern shelf areas, LIW consequently forms a single uniform water-mass from surface to sea floor. Exposed at the surface, upwelled LIW is directly affected by the regional climate as it travels northward. During winter, the Aegean Sea surface is exposed to cold and dry northerly outbreaks of polar/continental air masses, which cause strong surface buoyancy loss through cooling and evaporation (Theocharis and Georgopoulos, 1993).

1.3.) Current circulation pattern

The circulation pattern of the Aegean Sea has been described analytically in the past through series of observational and modeling studies and, according to Zervakis et al. (2004), it can be summarized as follows:

A branch of the westward-flowing Asia Minor current carrying warm, highly saline waters from the Levantine, enters the Aegean through the eastern straits and follows a northward track. The northward current along the Turkish coast of the Aegean mostly carries the Levantine Surface Water (LSW) mass and Levantine Intermediate Water (LIW) mass, extending from the surface down to 400 m. It forms an intense thermohaline front with the Black Sea outflow above the Lesvos shelf, thus forcing the Dardanelles jet. There, the Levantine waters get subducted below a thin surface layer of low-salinity modified Black Sea Water (BSW). Thus, the vertical structure of the water column in the north Aegean is comprised of a 20–70 m thickness surface layer of modified BW; below it an intermediate layer of Levantine waters (mostly LIW) extending down to 400 m; and a deep-bottom layer of locally formed North Aegean Deep Water (NAeDW), of distinct characteristics in each sub-basin. The surface and intermediate layers follow the general cyclonic circulation of the Aegean and gradually mix together as they flow southwards along the east coast of the Hellenic peninsula. By the time they have reached the south Aegean, these waters are characterized by significantly lower salinities than the northward-flowing Levantine waters in the eastern Aegean. These waters exit the Aegean through the western Cretan Arc Straits.

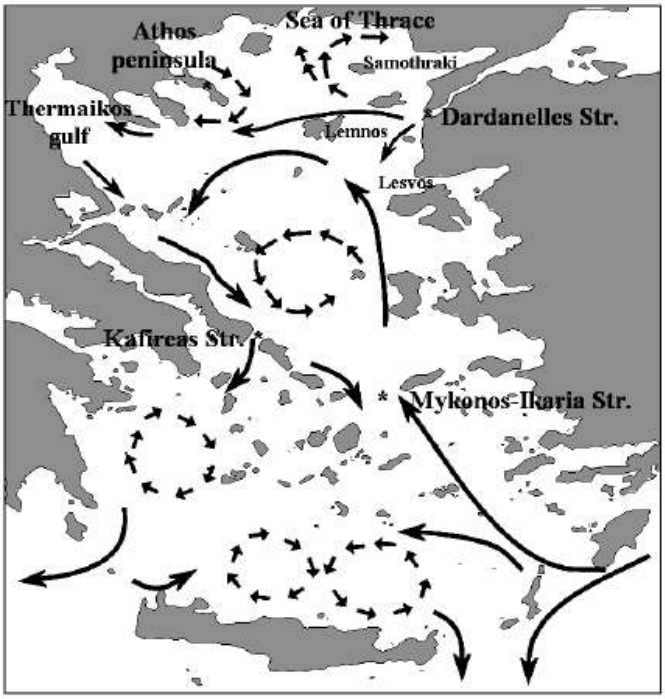

Fig.2: Schematic representation of the Aegean Sea upper circulation (from Nittis and Perivoliotis, 2002).

In the south Aegean, the surface layers consist of highly saline waters of Levantine origin, along with lower salinity Atlantic Water (AW) or signatures of BSW. Below the surface, the depths of approximately 50–300 m are occupied by annually ventilated Cretan Intermediate Water (CIW), similar to the LIW with slightly higher salinities. Below the CIW/LIW layer there is a core of Transition Mediterranean Water (TMW, currently down to 600–700 m depth), a water mass emerging from the mixture of LIW and Eastern Mediterranean Deep Water (EMDW) types and originating in the Levantine and Ionian basins (Balopoulos *et al.*, 1999; Theocharis *et al.*, 1999). Finally, the deep and bottom layers of the Cretan Sea are filled with dense Cretan Deep Water (CDW). The TMW mass enters the south Aegean through the Cretan Arc Straits to balance the outflow of surface and CDW.

1.4.) Deep-water formation and stagnation periods

According to many studies (e.g. Nielsen, 1912; Plakhin, 1972; Theocharis and Georgopoulos, 1993; Zervakis et al., 2000), the North Aegean is considered as a region of deep water formation of the Mediterranean. The deep sub-basins of the North Aegean, separated from each other and from the South Aegean by 350–400m deep shelves, are filled with extremely dense water, with recorded potential density exceeding σ_θ=29,63 kgm^{-3} (Zervakis et al., 2000). The communication between the North and South Aegean is free above the 400m isobath, and thus the intermediate layer of the North Aegean is filled with water of Levantine origin. The fact that the deep waters of the South Aegean are much lighter than those of the North Aegean certifies that, the latter are locally formed. In a study of the evolution of the North Aegean water columns through the late 1980s/early1990s, Zervakis et al. (2000) showed that incidents of local formation of very dense waters in the North Aegean took place in the winters of 1987 and 1992/ 1993 (**Fig.3**.)

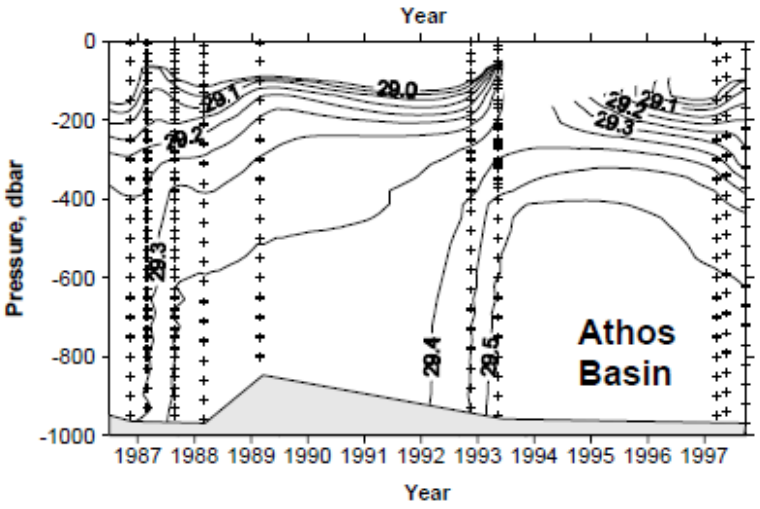

Fig.3.)Density contours versus time and depth in the Athos Basin of the North Aegean (Zervakis et al., 2000)

However, Zervakis et al. (2000) indicated that dense water formation events in the North Aegean demand large exchange of buoyancy with the atmosphere and also a significant reduction of the surface isolation lid, thus a reduction of the water surplus of the Black Sea. The Black Sea basin is a dilution basin, characterized by surface salinities less than 20. Its surface layer at the Straits flows towards the highly saline Mediterranean (S> 38), with the subsurface layer flowing towards the Black Sea. This flow is hydraulically controlled, and as a result of the increased mixing along the Straits, the salinity at the Aegean exit of the Dardanelles reaches about 28 (Ünlüata et al., 1990). Still, the salinity difference with the surrounding Aegean waters causes such a density difference, that the modified Black Sea water plume generates a thin (about 20 m) surface layer that covers the majority of the North Aegean (Zodiatis, 1994). Zervakis et al. (2004) suggested that the surface layer of the North Aegean is an effective isolator between the deep layers of the North Aegean and the atmosphere, absorbing large amounts of heat and buoyancy and hindering dense water formation. This combination of factors necessary for deep water formation in the North Aegean (large exchange of buoyancy with the atmosphere and significant reduction of the surface isolation lid) reduces the frequency of such events. During periods between dense-water formation events, the deep water properties of these basins are expected to change slowly, relaxing towards more homogeneous vertical profiles of temperature and salinity through their interaction with the overlying intermediate water masses. Considering that these basins are practically isolated below the 400m threshold, the main mechanism of this change is expected to be vertical diffusion through turbulent mixing, according to Zervakis et al. (2003). The latter authors suggest that the critical breaking of internal waves is a very possible reason for more intense mixing.

The aforementioned work (Zervakis et a., 2003) is based on series of CTD casts from three deep sub-basins of the North Aegean. As the temporal distance between successive casts at the same position in that data set ranges from several months to (more commonly) a few years, the estimations of effective eddy diffusivity correspond to processes time scales of a year of more. Recent numerical simulations by Mamoutos et al. (personal communication) indicate the possibility, that an annual cycle might be overlaid on the interannual density decay of the deep basins during stagnation periods. However, this result is highly depended on the selection of a vertical advection scheme as well as the selection of a turbulence closure scheme. Thus, it is imperative to use new high-frequency data from the deep layers of the North Aegean in order to examine the behavior of the basin at shorter-than-annual time scales.

A golden opportunity to investigate this question rose in 2015, when a profiling ARGO float was trapped (probably by topographic steering of the flow) within a deep sub-basin of the North Aegean, the North Sporades basin, and remained there for about a year. This work exploits the ARGO-derived hydrographic profiles in order (a) to examine whether there is an annual cycle recorded in the deep basins and (b) to produce vertical eddy diffusivity estimates, representing phenomena of shorter time-scales.

Thus, below, the data and methodology used are presented in the following chapter 2.). The results are presented in chapter 3.) and are summarized and discussed in the concluding chapter 4.).

2.) Data and Methods

2.1.) MedArgo profiling float data

The principal source of data for this study comes from temperature and salinity profiles collected by the MedArgo float sensor nr. 6901884, which has been trapped in the Athos–Sporades Basin of the North Aegean Sea. All available data, from 07.10.2014 up to 26.11.2015, belong to the GreekArgo infrastructure as part of the EuroArgo ERIC and were downloaded from the Coriolis Global Data Assembly Center site (ftp://ftp.ifremer.fr/ifremer/argo/). A total of 154 samples between 19–25◦ E and 38–41◦ N (Figure 4.) were analyzed, using the programs MATLABR2015a and Ocean Data View 4. For calculation and use of thermodynamic properties the Gibbs Seawater (GSW) Oceanographic Toolbox was downloaded and used, following the instructions by IOC. (2010).

The float data are processed and archived in near-real time at the CORIOLIS Data Centre and are distributed on the GTS following the standards of the international Argo program. MEDARGO full datasets can be viewed and downloaded in quasi-real time from CORIOLIS (http://www.coriolis.eu.org/cdc/projects/cdcMFSTEPFloats.asp). Float trajectory plots are also produced in near-real time at the MEDARGO Thematic Expert Data Center (OGS, Trieste) and can be viewed at http: //doga.ogs.trieste.it/WP4/real_time.html.

2.1.1.) Quality control

To ensure the accuracy and reliability of these data, quality control was made following the Argo Quality Control Manual (Wong et al., 2015). This progress included controlling the platform identification, the appearance of impossible date and location, positions on land and regional water mass characteristics range for the Mediterranean Sea. The used temperature and salinity profiles are represented in Figure 5.)

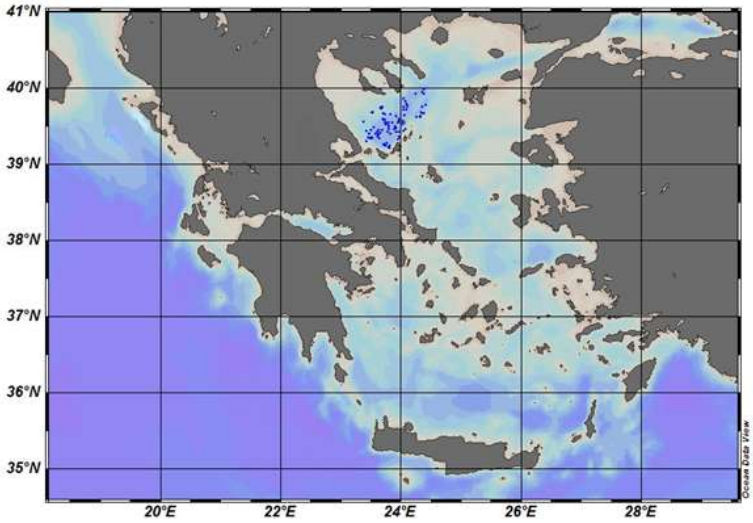

Figure 4.) Geography of the study area: the float positions are indentified by blue bullets

2.2.) NCEP/NCAR Air-Sea flux data

Air-sea flux data come from the National Center for Atmospheric Prediction (NCEP) and the National Center for Atmospheric Research (NCAR) daily reanalysis and were used to examine time-series of air-sea fluxes and heat loss (sea to air heat flux) in the region of the examined ARGO float locations during the years 2014 and 2015. The air-sea flux data represents the net of: incoming solar radiation, back radiation, latent and sensible heat loss.

2.3.) EMODNet bathymetry data

The bathymetry data have been derived from the European Marine Observation and Data Network (EMODnet) Bathymetry portal (http://www.emodnet-bathymetry.eu.).The processed and quality controlled digital bathymetry data have been used in order to estimate the surface and the volume of the Athos Basin within the deep layer from the top of the considered layer z to the bottom D.

2.4.) Estimation of the stratification frequency

The stratification frequency, known as Brunt–Väisälä frequency (Eq. (1)), has been used as an index of the stratification between the intermediate and the deep layers. For that purpose, the stratification frequency was estimated within the layer between 300 m and 400 m, which is located around the minimum depth of the deep basins' rims.

$$N^2 = \frac{\left(-\frac{g}{\rho_0}\right) * (\rho_1 - \rho_2)}{\Delta z} \quad (1)$$

g: gravitational acceleration (9,806 m/s2),

ρ_0: initial ambient sigma–theta (1022,4 kg/m3),

ρ_1: upper layer(300-400m) mean density, ρ_2: lower layer(400-500m) mean density,

Dz: equal to 100 m in order to calculate the stratification frequency in the 300–400 m layer

2.5.) Estimation of the eddy diffusion coefficient

In order to estimate the vertical diffusion coefficient K_c, the methodology from Zervakis et al. (2003) has been used. According to this method the advective terms can be neglected within the deep basin. This is due to the fact that lateral diffusion is a much faster process than vertical diffusion and over the time-scale of a year is expected to laterally homogenize the selected deep-basin. In the present case of the ARGO float, the advection terms are naturally neglected due to the Lagrangian nature of the measurement. It can be assumed that vertical mixing dominates over lateral diffusion in determining the evolution of the properties of a deep water body. The fact that there is no mean vertical motion during stagnation periods eliminates the vertical upwelling and convection term. Furthermore, horizontal integration throughout any whole horizontal surface at depths below 400m eliminates the horizontal advection terms. After vertically integrating within the deep layer from the top of the considered layer z to the bottom D, the equation below (Eq. 2) can be obtained as follows:

$$\bar{A}(z)\frac{\partial \bar{c}(z)}{\partial t} = \frac{1}{(z-D)} * \left\{ \left| A(z)K_c(z)\frac{\partial c}{\partial z}\right|_z - A(D)K_c(D)\frac{\partial c}{\partial z}\right|_D \right\} \quad (2)$$

$$with \qquad \bar{c}(z) \equiv \frac{1}{(z-D)\bar{A}(z)} \int_D^z A(\zeta)c(\zeta)d\zeta \quad (3)$$

$$and \qquad \bar{A}(z) \equiv \frac{1}{(z-D)} \int_D^z A(\zeta)d\zeta \quad (4)$$

$\bar{c}(z)$ and $\bar{A}(z)$ are defined as the mean integrated values of c and A from depth z to D. The physical interpretation of the equation above is, that the change of the mean value of the property c within a layer of water equals the net input through the top and bottom of the layer.

Since the change of hydrological characteristics of the considered water mass is consistent with vertical mixing (due to the fact that the properties of the deeper water masses slide along the θ-S curve towards lower densities as shown in figure 8.), the equation above (Eq 2.) can be solved for the eddy diffusion coefficient K_c:

$$K_c(z) = (z-D)\frac{\bar{A}(z)\partial\bar{c}}{A(z)\partial t} \left(\frac{\partial c}{\partial z}\Big|_z\right)^{-1} + K_c(D)\frac{A(D)}{A(z)} \frac{\partial c}{\partial z}\Big|_D \left(\frac{\partial c}{\partial z}\Big|_z\right)^{-1} \quad (5)$$

And considering the fact that the flux at the bottom of the basin is zero, the eddy diffusion coefficient $K_c(D)$ can be ignored and equation 5 can be simplified as folows:

$$K_c(z) = (z-D)\frac{\bar{A}(z)\partial\bar{c}}{A(z)\partial t} \left(\frac{\partial c}{\partial z}\Big|_z\right)^{-1} \quad (6)$$

3.) Results

The trapped MedArgo float sensor nr. 6901884 provided high frequency observations in the Athos–Sporades Basin of the North Aegean Sea, which have been used to estimate the vertical and seasonal hydrographic characteristics of the different water mass layers. The atmospheric and water masses heat flux, the mixed layer depth, the vertical stability and the vertical diffusion were estimated in order to determine the deep-water stagnation period and to examine the vertical mixing. Since the vertical eddy diffusion coefficient K_S (based on the observed rate of change of salinity) indicated a possible sensor drift of the specific float, corrections in order to calibrate the conductivity sensor were made before the final estimations of the eddy diffusion coefficients $K_{\sigma\theta}, K_S, K_T$.

3.1.) Hydrographic characteristics

The temperature, salinity and potential density anomaly characteristics measured during 2014-2015 are depicted in Figure 5.) and Figure 6). The projected data in the following θ-S diagram (Fig. 7.) revealed that the Θ-S values lie more or less on the same curve throughout the examined period and that the properties of the deeper water masses slide along this curve towards lower densities.

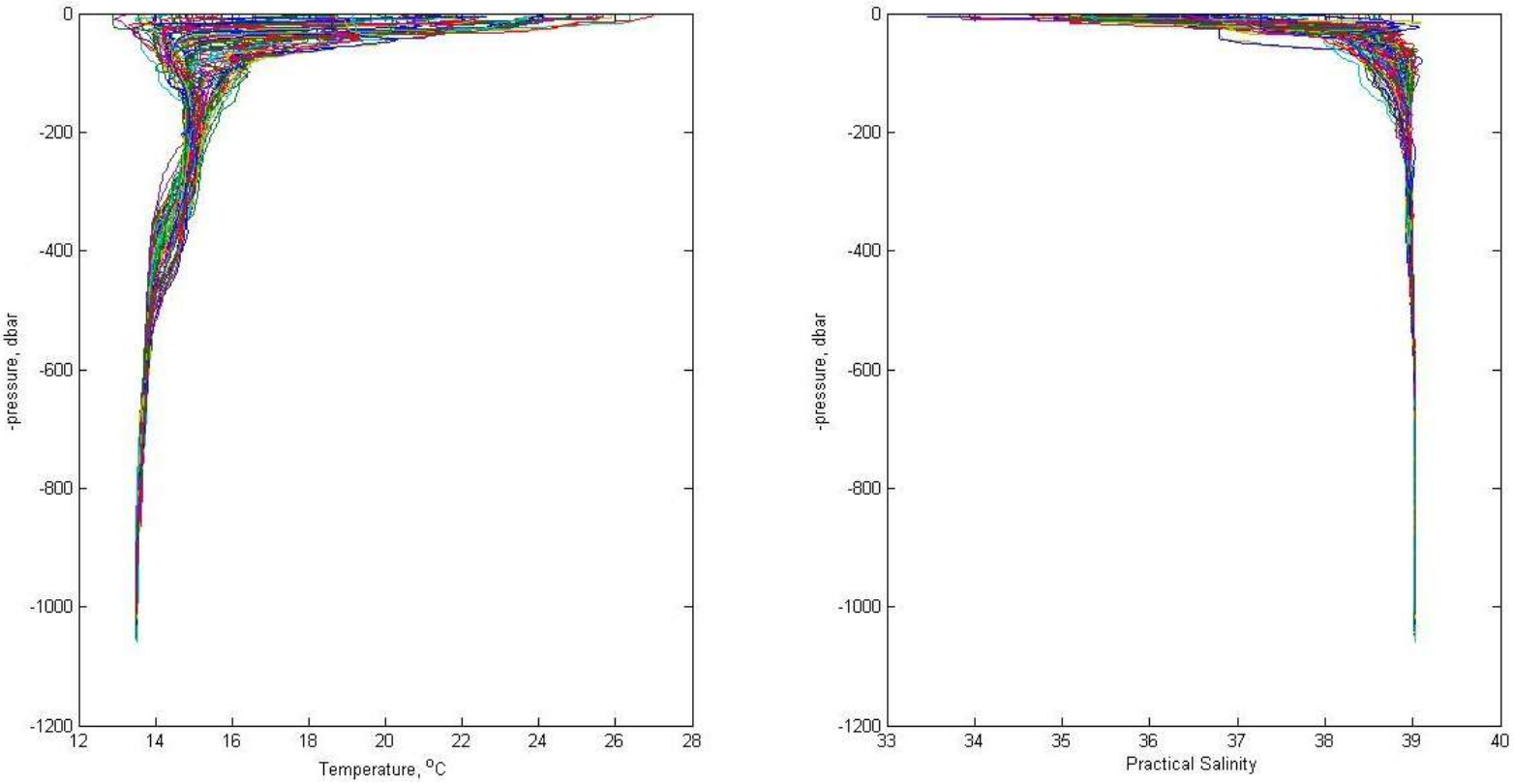

Figure 5.) Temperature and salinity profiles collected by the MedArgo float sensor nr. 6901884

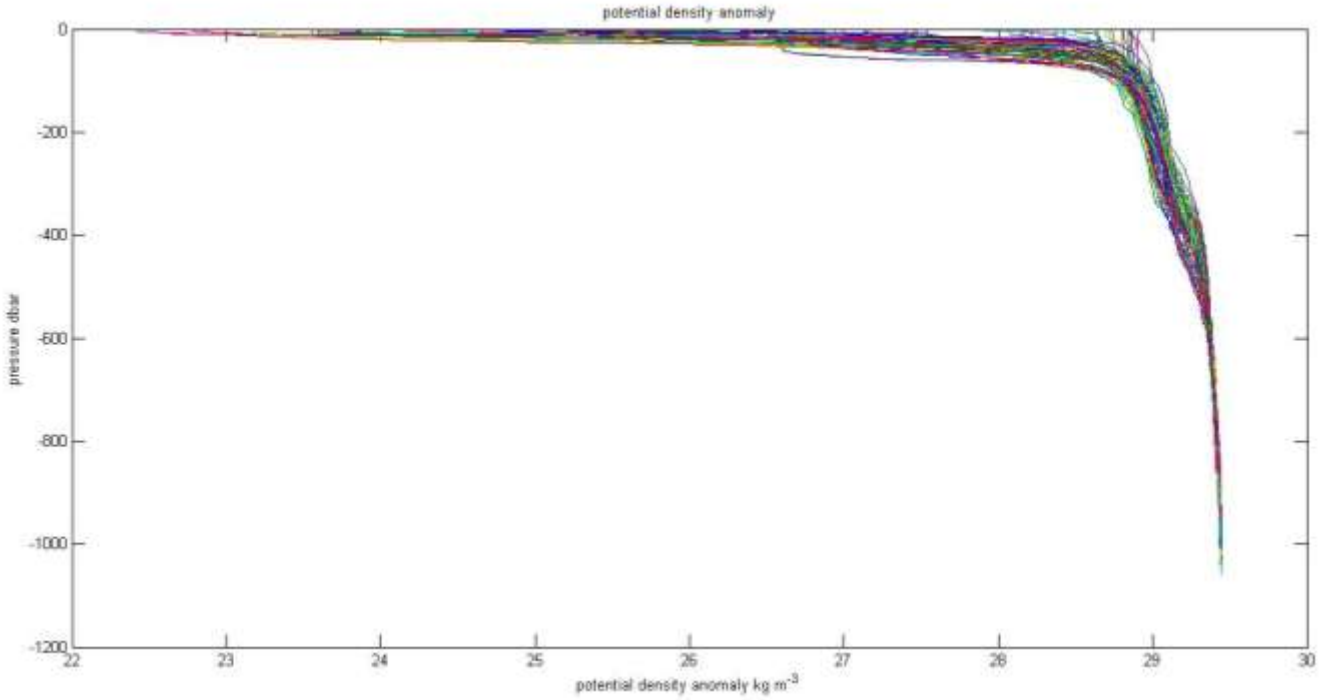

Figure 6 .) Calculated potential density anomaly versus pressure

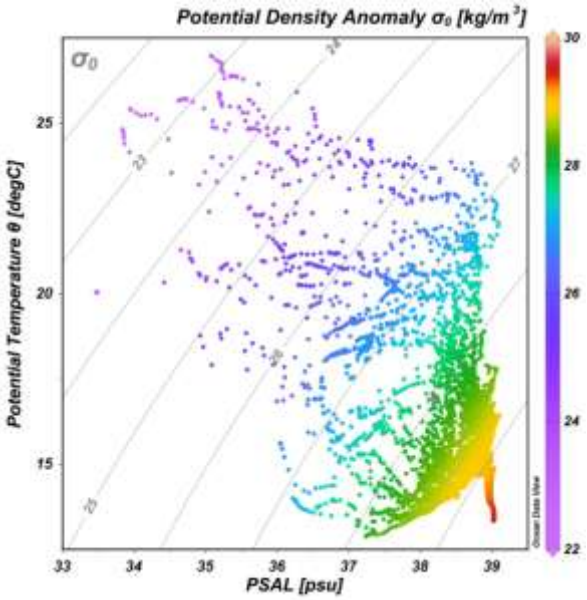

Fig. 7.) Diagram θ-S for all data set

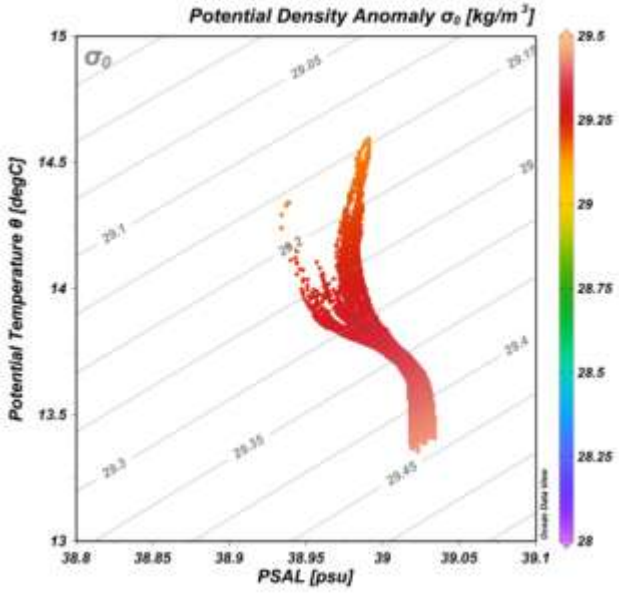

Fig.8.) Diagram θ-S for the deeper-than 400m water masses

The right θ-S diagram (fig.8.) reveals that the Θ–S deep-water (>400m) values lie on the same curve throughout the examined period, which indicates that the deep-water mass properties slide along this curve towards lower densities. According to Zervakis et al. (2003), this is a proof that vertical diffusive mixing is the dominating mechanism for this relaxation, as the bottom layer exchanges mass with the upper layer.

3.1.1.) Vertical variability

In the Athos-Basin, three layers of distinct water masses with very different properties were observed, following the description from Zervakis and Georgopoulos (2002):

i) The up-to-50m thick surface layer, which is occupied mainly by Black Sea Water, as seen in figures, is characterized by a maximum temperature of T=25°C, a minimum salinity of S=35 and a minimum potential density anomaly of σ_0=24kgm^{-3}.

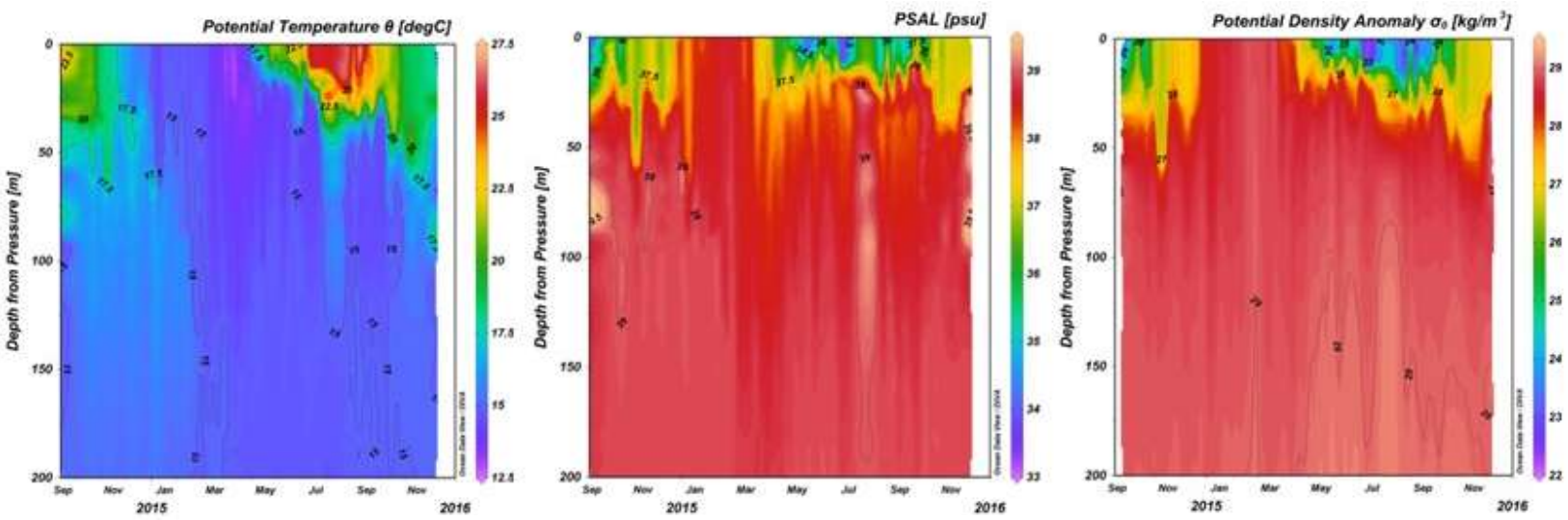

Fig. 9.) Potential temperature, salinity and potential density by depth evolution (Sept 2014–Nov 2015) in the surface layer

ii) The intermediate layer, extending down to 400m depth, with a maximum temperature of T=16°C, salinity up to S=38,6 and potential density anomaly up to σ_0=29,1 kgm^{-3}.

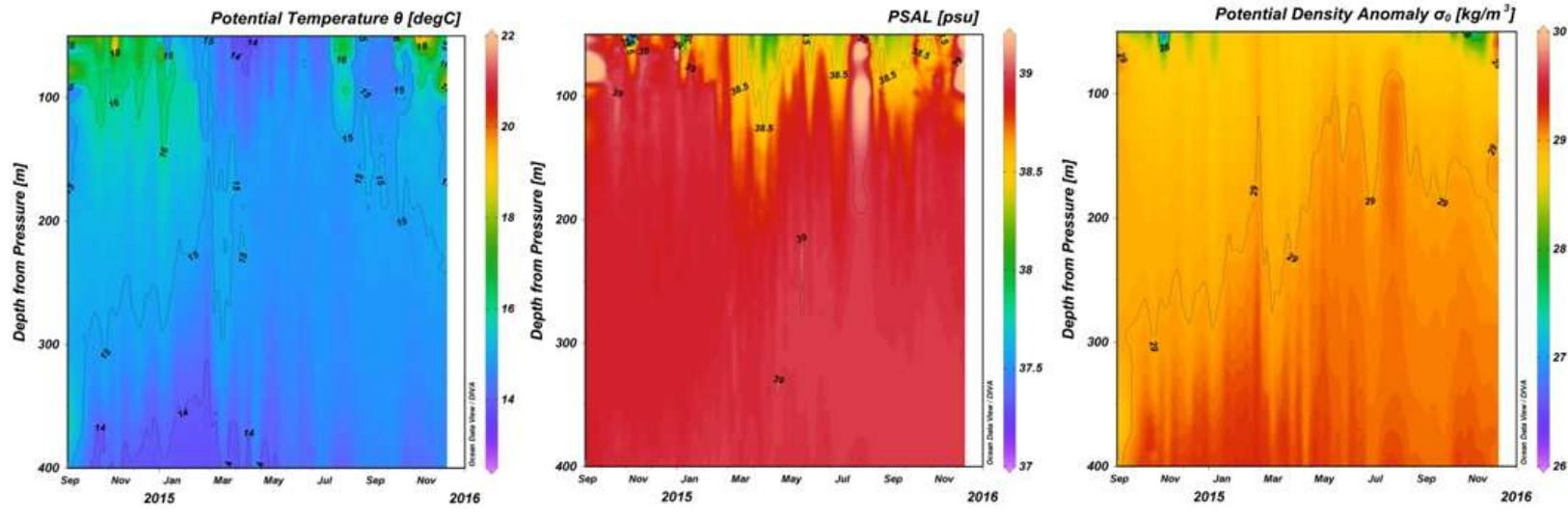

Fig.10.) Potential temperature, salinity and potential density by depth evolution (Sept 2014–Nov 2015) in the intermediate layer

iii) Below this layer, the deeper-than-400 m basins of the North Aegean contains very dense water with salinity reaching S=39, temperature values under T=14,5°C and potential density anomaly up to σ_0=29,4kgm^{-3}.

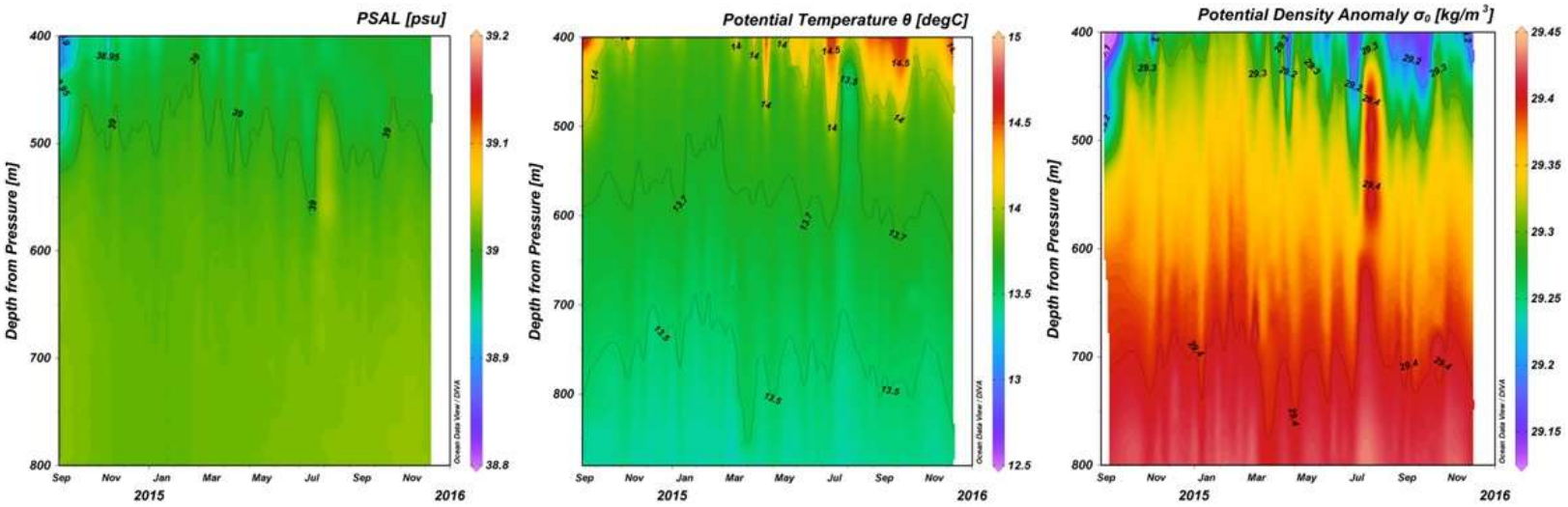

Fig.11.) Potential temperature, salinity and potential density by depth evolution (Sept 2014–Nov 2015) in the intermediate layer

3.1.2.) Seasonal variability

The seasonal variability of the upper layers of the North Aegean seems to be prominent in all figures (Fig. 9.).The surface waters in March are much colder than the rest of the water column. Although the influence of the inflowing BSW is mainly confined to the surface layer, the lower layers are eventually affected. The seasonal cycle is evident with maximum salinity values during winter, when the BSW inflow is the lowest. Reduction of salinity throughout the spring and minimum values at the end of summer are related with the maximum BSW spreading in the basin. Due to surface heating, the thermocline develops from May and peaks during July-August. During the winter period temperature values at the surface are lower than those of the underlying layers (Fig. 9). But this does not lead to instability due to the low salinity values of the surface layer. The low surface salinity relates to the presence of BSW, which reaches the Athos area brackish surface water mass (Zodiatis, 1994). The presence of low salinity BSW at the surface hinders the dense water formation ability of the Northern Aegean. This surface layer can lose significant amounts of buoyancy during cold winter events without becoming dense enough to form deep waters (Zervakis et al., 2000).

In early autumn the water column gradually looses heat. From January to March it seems to become homogenized in the upper 100m. In the particular area and for the particular time period, winter homogenization did not penetrate far below the first 100 m layer, as densities in this surface layer during the peak of homogenization did not exceed 29 kgm^{-3} (Fig.12.).

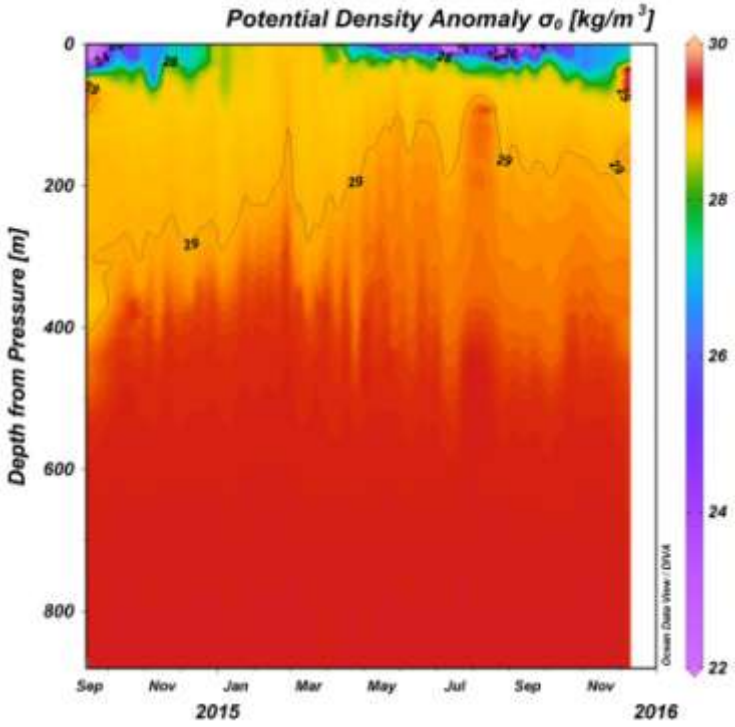

Fig.12.)Potential density by depth evolution: winter homogenization within the upper ~120 m

The density in the first 100m is less than the density of the underlying intermediate water masses, which is more than 29 kgm^{-3} (Fig.12.). The 100m depth is not at the core of the intermediate layer in the North Aegean, according to Velaoras and Lascaratos (2010), but it can be assumed, that it is the upper limit of this layer. So the changes in the characteristics of the 100m layer can be linked to respective changes of intermediate layer characteristics. As a result, the salinity increase observed after the end of winter and up to the end of autumn is followed by an increase in temperature starting at the end of spring up to the beginning of winter.

3.2.) Heat Flux

During summer (July–August) and winter (December–February) strong winds from northern directions hit the Aegean Sea. These northerly winds bring relatively cold continental air from Southern Russia and the Caspian Sea, contributing to the decrease of surface temperature and the moderation of summer heat that leads to surface buoyancy loss (Poulos et al., 1997). Dense water formation at the surface is related to the buoyancy flux, which is determined by the heat and freshwater fluxes between the atmosphere and the sea. The sinking of the dense surface water to the intermediate and the deep layers is also connected with the stability of the stratification of the water column. Papadopoulos et al. (2012) underline that intermediate and deep water formation is directly related to extreme winter heat loss events. Due to its small size, the Aegean Sea surface should respond rapidly to the meteorological changes and the variability of the lateral fluxes. This variability propagates in the thermohaline characteristics of the deep water masses of the basin through deepwater formation processes.

The graph below (Figure 13) represents air-sea flux data from the National Centers for Atmospheric Prediction (NCEP*)* and the National Center for Atmospheric Research (NCAR). This time series were used to estimate the air to sea heat flux in the region of the examined ARGO float locations during the years 2014 and 2015.

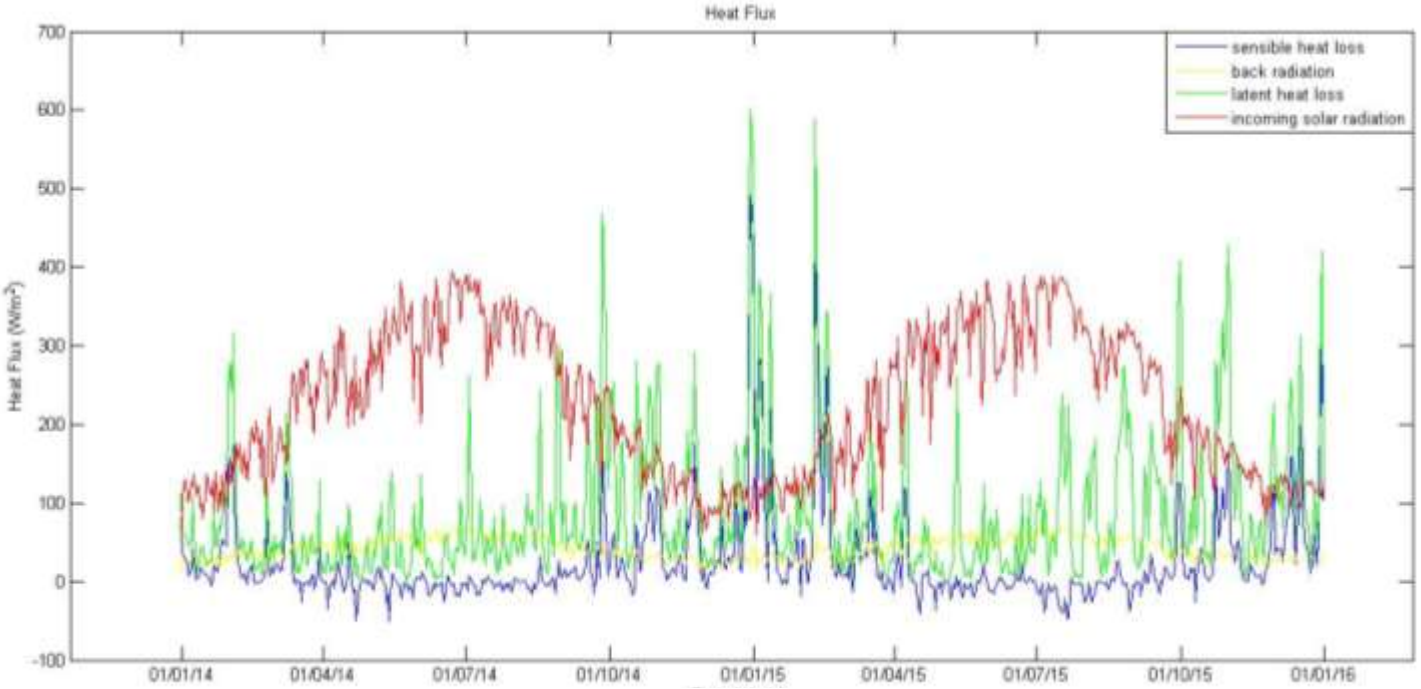

Figure 13.) Seasonal evolution of air-sea flux data from the National Centers for Atmospheric Prediction (NCEP) and the National Center for Atmospheric Research (NCAR). Positive values represent upward heat flux (heat loss by the sea), except in the case of solar radiation.

The flux data represents the net of the incoming solar radiation, back radiation, latent and sensible heat loss:

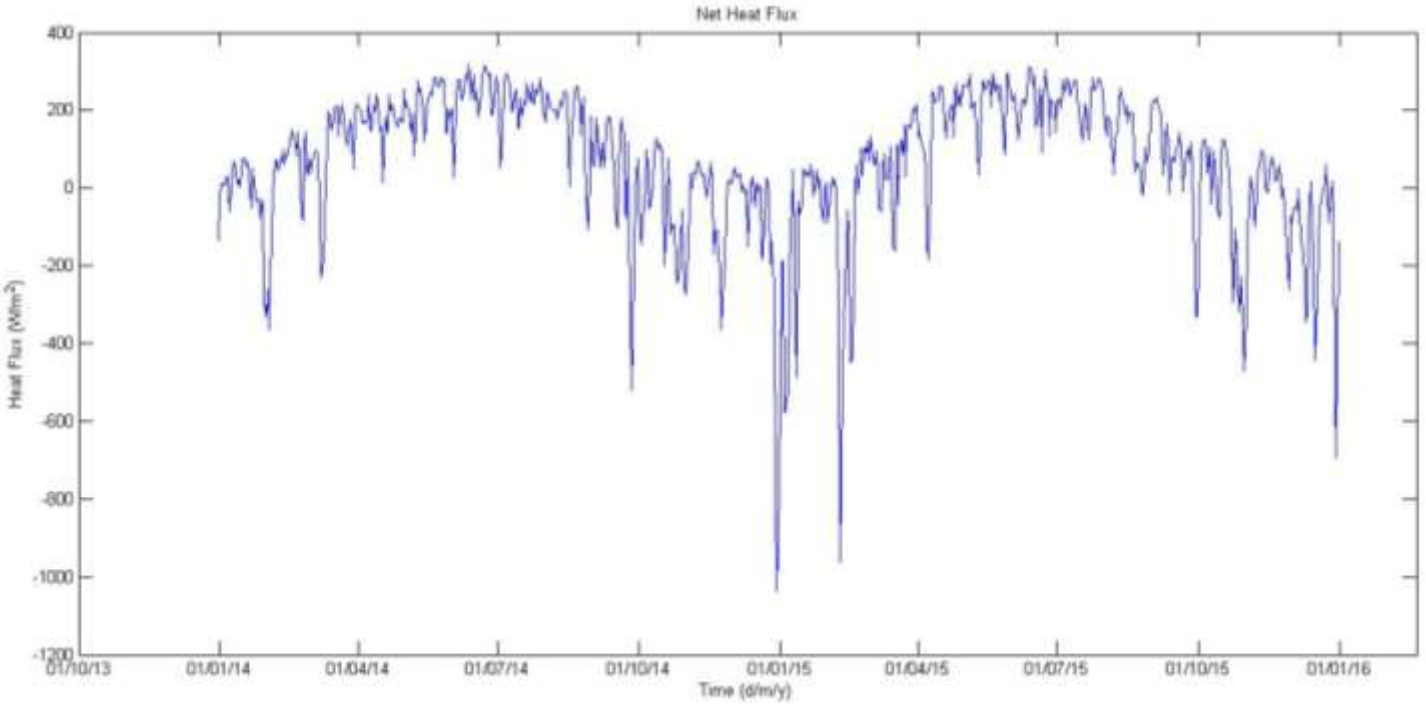

Figure 14.) Seasonal evolution of net heat flux from the sea surface in the North Aegean. Here, positive values indicate heat gain by the sea.

The winter heat flux from the sea surface in the North Aegean shows an intense variability. Extreme values of heat loss were observed during January, February and March 2015 . The maximum heat gain can be seen during June and July. A seasonal dominant dense deep-water formation seems possible to occur during the winter of 2015, since dense water formation is expected to occur during high frequency heat loss events.

3.3.) Mixed layer depth

The atmospheric and water masses interactions control the air–sea buoyancy balance and the characteristics of the mixed layer formation. Both are related to the formation of denser waters. The ocean mixed layer is characterized by nearly uniform physical properties throughout the layer with a gradient of properties at the bottom. The mixed layer links the atmosphere to the deep ocean and plays a critical role in climate variability. Atmospheric fluxes of momentum, heat and freshwater through the ocean surface drive vertical mixing that generates the mixed layer. The depth of the mixed layer varies with time due to the variability atmospheric forcing. The thickness of the mixed layer indicates the amount of water and heat that directly interacts with the atmosphere. The evolution of the seasonal mixed layer is influenced by a variety of phenomena, including air-sea heat flux (Yu and Weller, 2007), air-sea freshwater flux (Yu, 2011), air-sea momentum fluxes, continental, turbulent and convective mixing of water properties from below, the structure of the water properties below including barrier layers (de Boyer Montégut et al., 2007) and horizontal as well as vertical advection of water properties.

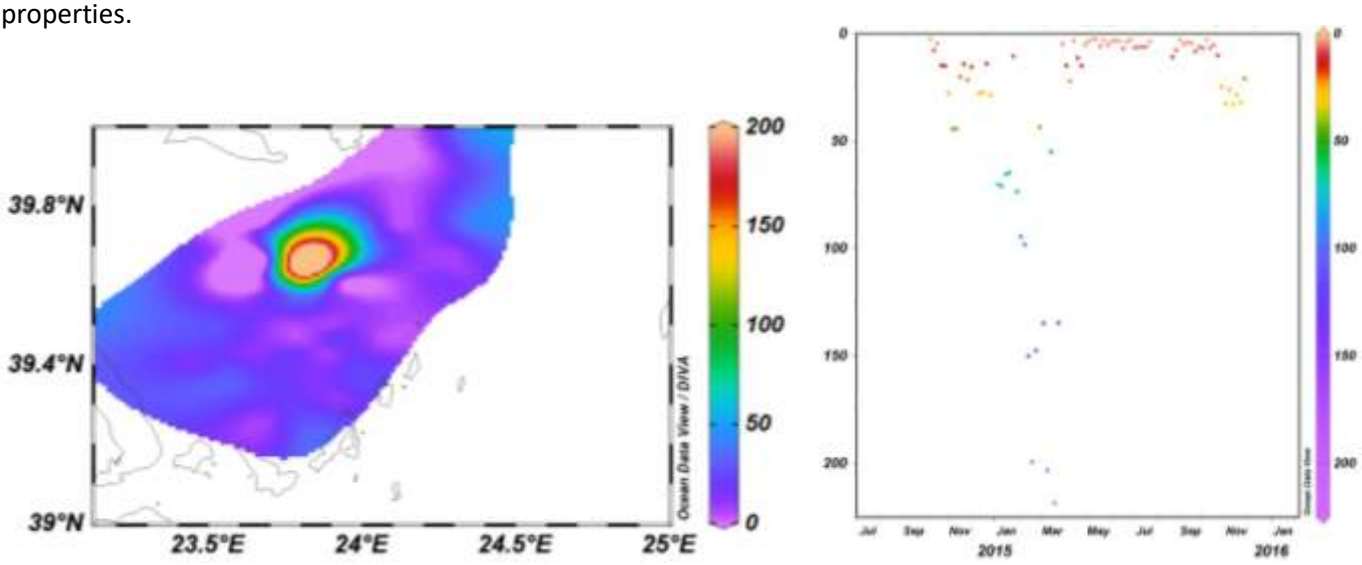

Fig.15.) Mixed layer depth versus longitude-latitude (left) and versus depth (right) evolution based on the density threshold (0,125 kgm^{-3}) criterion

The mixed layer depth seems to follow the seasonal winter homogenization structure. During winter the strong northerly winds bring relatively cold continental air which provides the necessary exchange of buoyancy with the atmosphere. But the surface layer of the North Aegean can be considered as an effective isolator between the deep layers and the atmosphere, absorbing large amounts of heat and buoyancy. So, we can assume that cold atmospheric events are not solely responsible for the formation of the observed dense bottom water. The high salinity values, which characterize the deep water type, lead to the assumption that augmented salinity is a precondition of deep water formations in the North Aegean.

This fact shows probably once again the condition of a significant reduction of the water surplus of the Black Sea, which hinders the dense water formation. This combination of necessary factors for deep water formation in the North Aegean reduces significantly the frequency of these phenomena.

3.4.) Vertical stability

Tragou et al. (2003) have shown that, during deep-water formation events, the intermediate layers of the Aegean can carry buoyancy northwards; thus, in order to balance the buoyancy budget, the surface layer would accelerate its southward buoyancy transport, concluding that massive dense water formation events in the north Aegean would significantly accelerate the thermohaline conveyor belt of the Aegean Sea. The formation of dense waters in the upper ocean and their transfer to intermediate and deeper depths is directly related to the level of the water column stratification. The existence of strong stratified layers in the bottom of the intermediate masses over the North Aegean deep basins is a deterrent factor on the intrusion of the new-formed dense waters into the basins. For this reason are represented below the values of the stratification frequency, known as Brunt–Väisälä frequency (Eq. (1)), which reveals the vertical mixing ability of the dense waters in the layer between 300 m and 400 m, which is located around the minimum depth of the deep basins' rims.

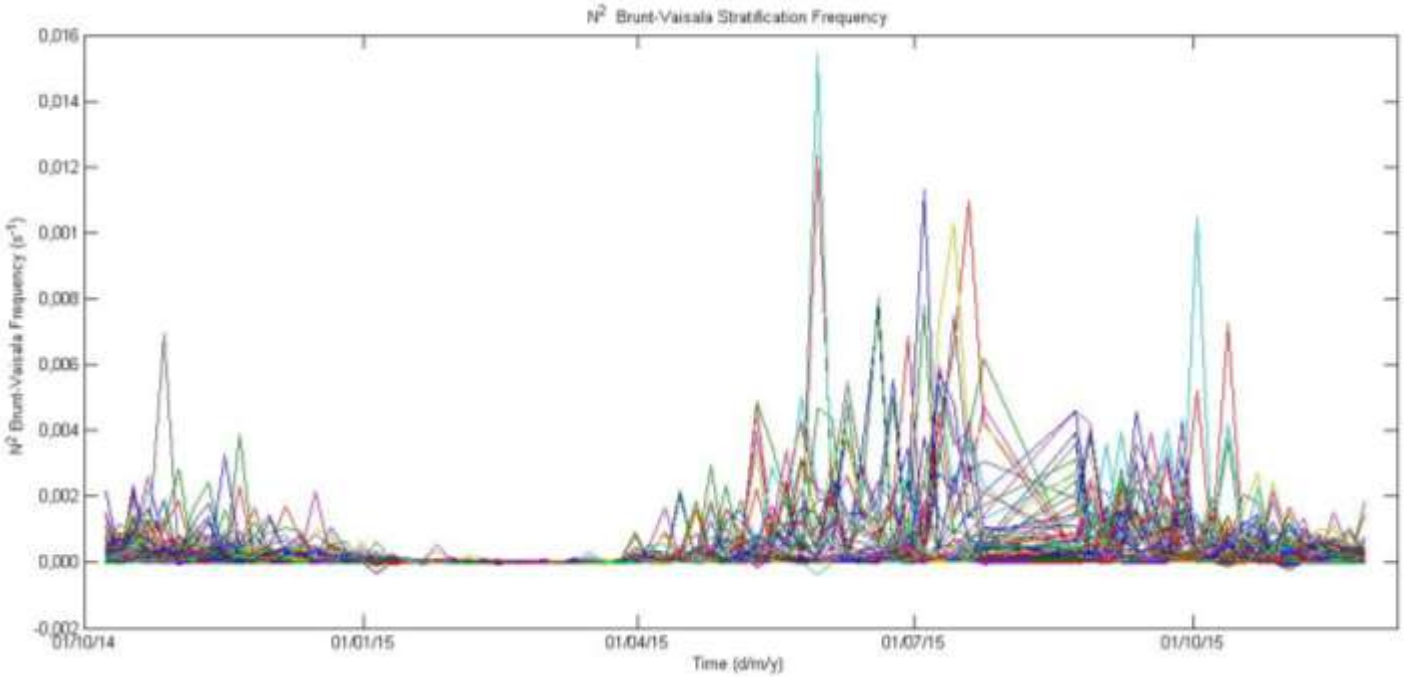

Fig.17.) Seasonal variability of the stratification frequency N^2

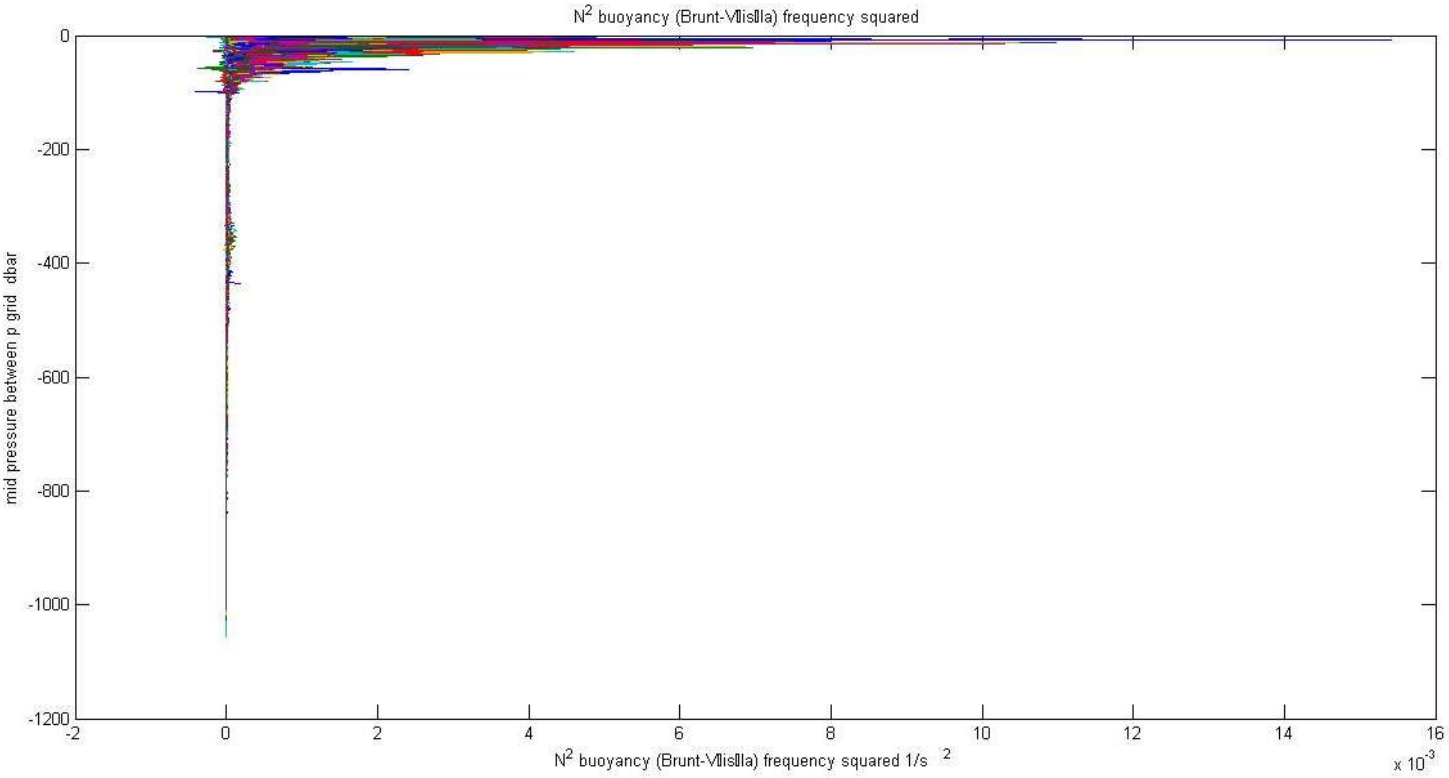

Fig.18.) Vertical variability of the stratification frequency N^2

High stratification frequency values seem to indicate strong stratification, low dense water formation activity, and weak vertical mixing ability toward deeper areas. It can be assumed that during the examined time range, possible mixing occur only within the upper, warmer and less saline layers.

3.5.) Vertical diffusion

Vertical diffusion estimations were made following the methodology by Zervakis et al. (2003), where the eddy diffusivity coefficient K_c has been estimated in order to describe the balance between the time rate of change of the vertically integrated concentration of a passive tracer in the stagnant basin and the divergence of the vertical diffusive flux of tracer through the upper and lower boundaries. According to the bibliography also Axell (1998) has used this method in estimating vertical diffusivities for deep sub-basins of the Baltic Sea during stagnation periods.

At first, according to the methodology described in chapter 2.5.), took place the vertically integration of the values of density, temperature and salinity within the deep layer from the top of the considered layer of 400m and 600m to the bottom of the basin. After the selection of the exact time span of the stagnation period (April-October: circles in Fig.19.) Spatially averaged potential density of the deeper than 400m and 600m layers it was possible to estimate the vertical gradient of the parameters around the interface(+/- 50m), which can be seen in the figures below (Fig.20.) ,Fig.21.) , Fig.22)):

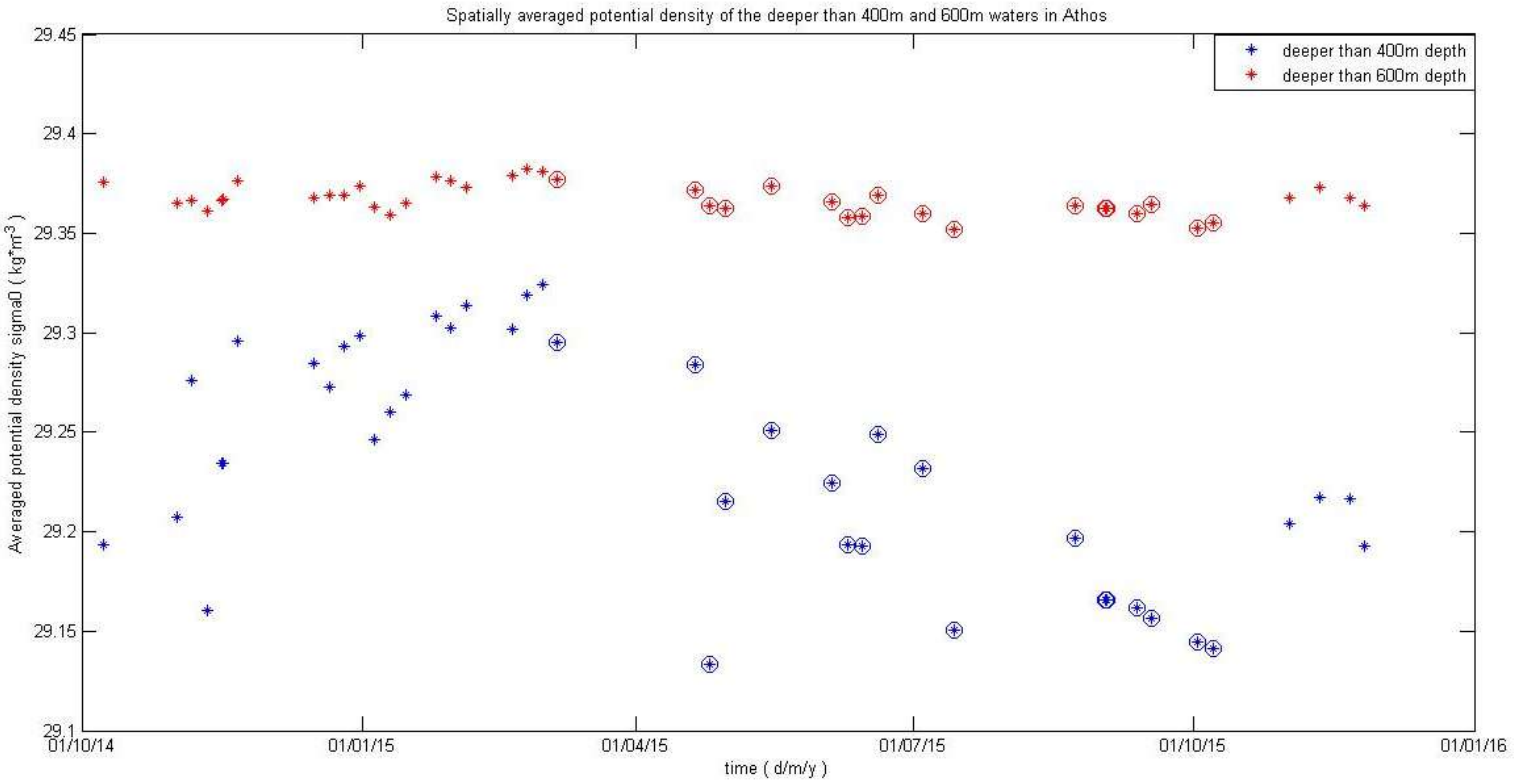

Fig.19.) Spatially averaged potential density of the deeper than 400m and 600m layers.
The points identified by the overlaid circles denote the temporal range of the stagnation period, from March till October 2015.

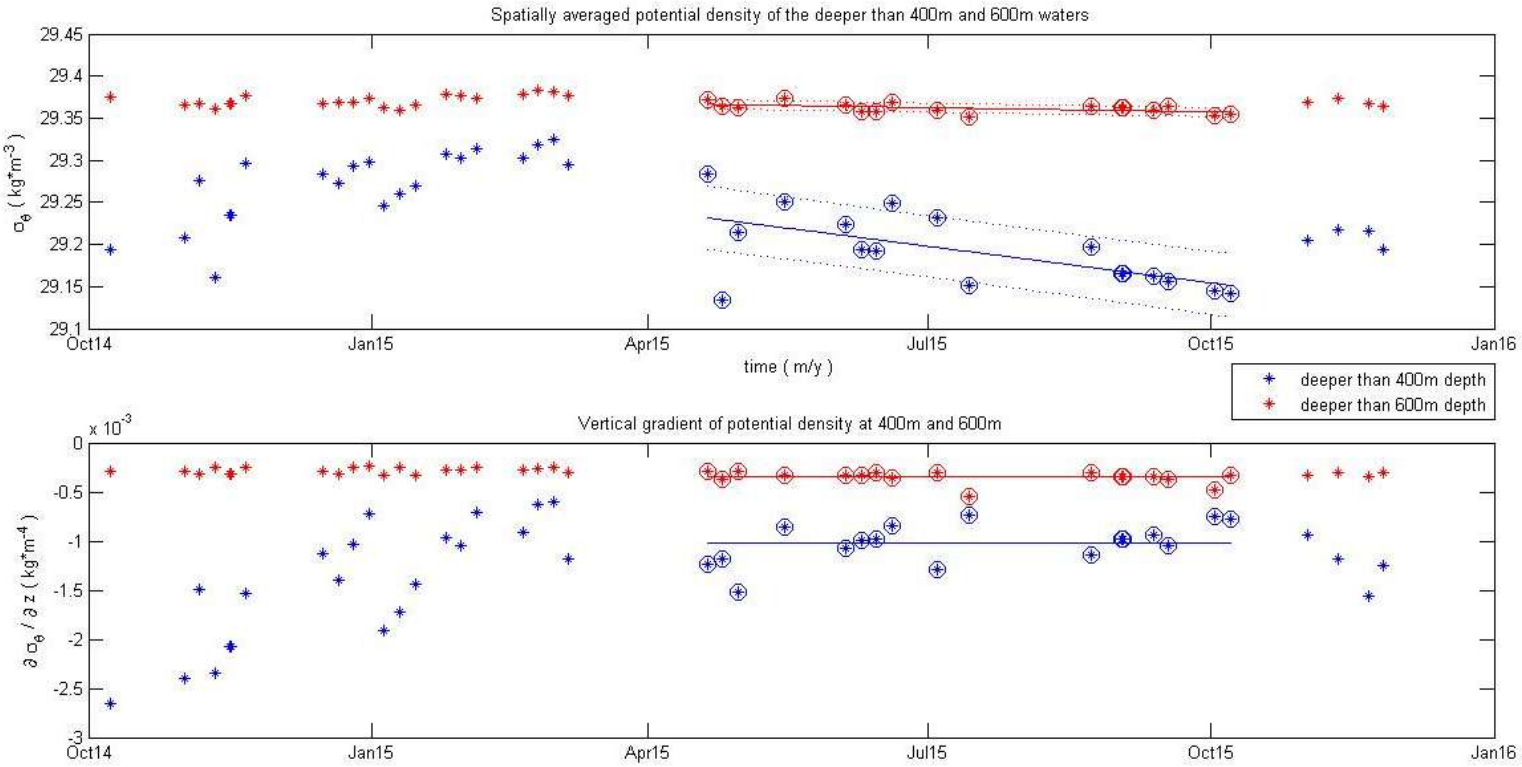

Fig.20.) Top: Spatially averaged potential density of the deeper than 400m and 600m layers
Bottom: Vertical gradient of potential density at +- 50m around the interface

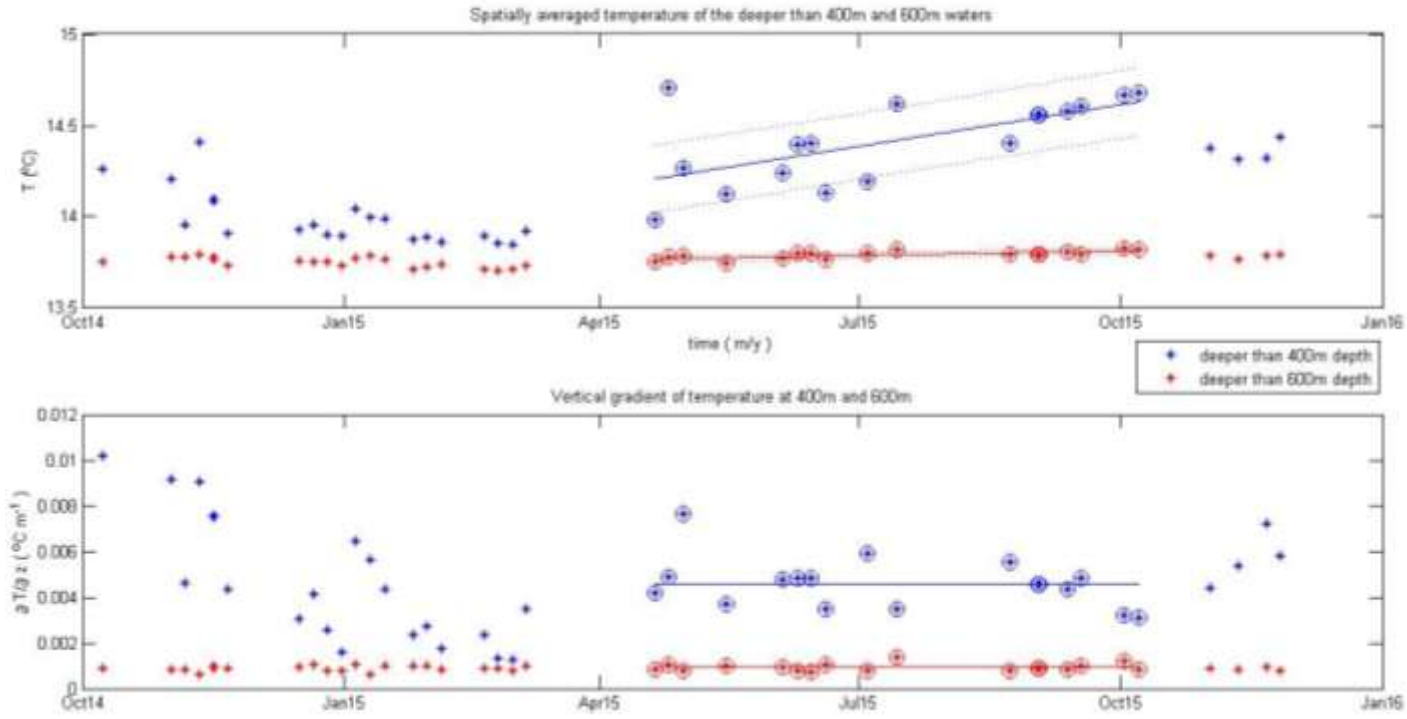

Fig.21.) Top: Spatially averaged temperature of the deeper than 400m and 600m layers
Bottom: Vertical gradient of temperature at +- 50m around the interface

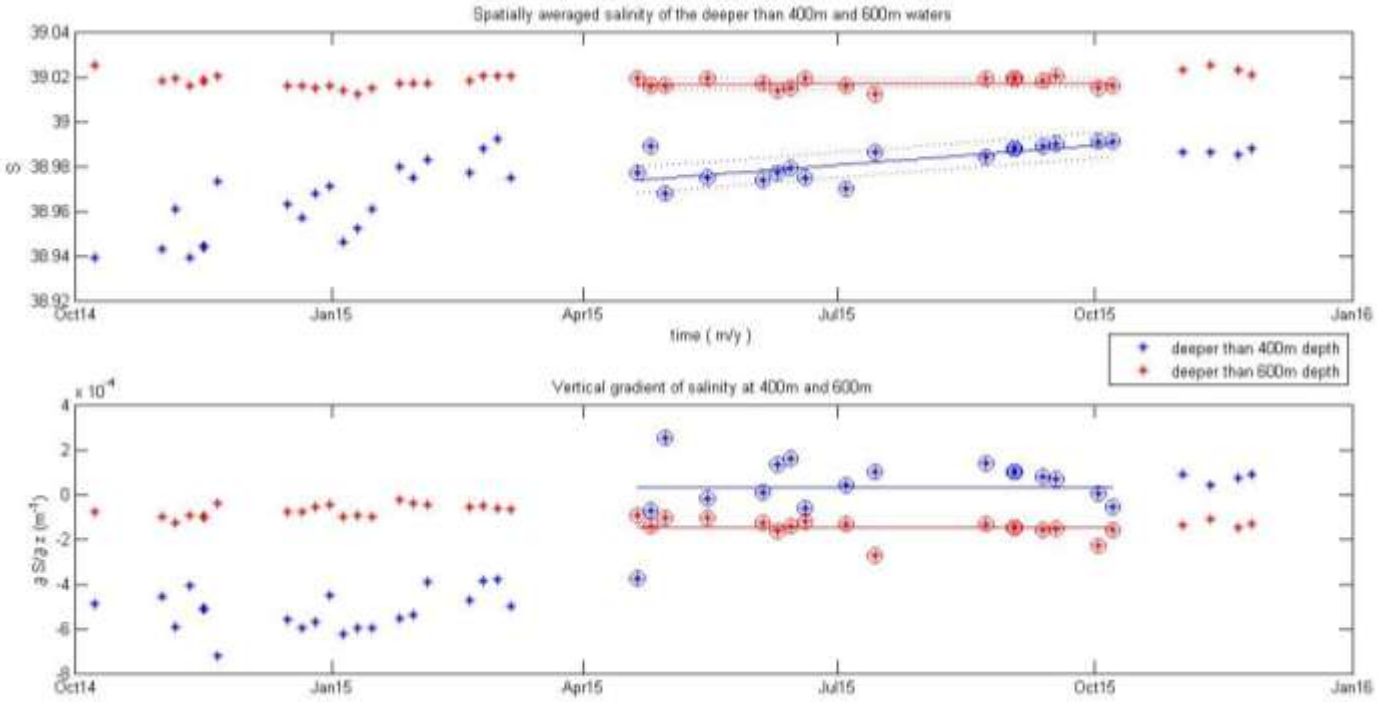

Fig.22) Top: Spatially averaged salinity of the deeper than 400m and 600m layers
Bottom: Vertical gradient of salinity at +- 50m around the interface

From the results above it can be seen that the temporal evolution of the simulated averaged potential densities reveals the expected "sawtooth" behavior only in the upper examined layer (waters deeper than 400m). According to Zervakis et al. (2003) the sharp rise of values at the beginning of the year, which seem to follow the heat loss peaks from the sea (Figure 14), are generated by the alternation of short-termed dense-water formation episodes and a longer-termed stagnation period. As is it seems, the water masses deeper than 600m remain almost constant, without being affected by the dominant seasonal cycle.

The hydrological characteristics changes of the basin have been examined before the actual estimations of the vertical eddy diffusion coefficient $K_{\sigma\theta}$, K_S, K_T . For that purpose the tool of the Θ/S diagram (Fig.23.) was employed within the stagnation period for the deeper than 400m layers. Unexpectedly it indicated some uncharacteristic salinity measurements, which might have been caused by drifting of the conductivity sensor:

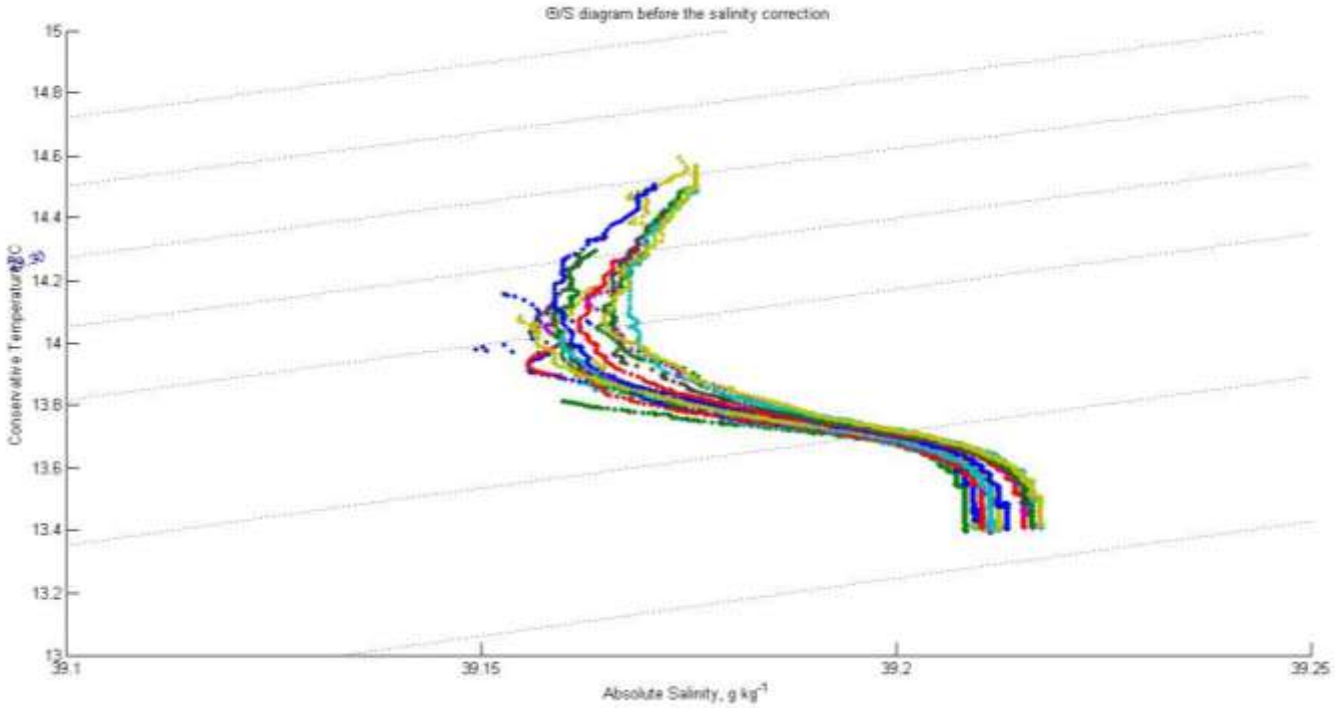

Fig.23.) Θ/S diagram within the stagnation period for the deeper than 400m layers

As it can be seen in the figure above, the profiles in the diagram seem to move along the salinity- axis. This does not agree with the process of mechanical mixing. The values should lie along the same curve throughout the whole period. The salinity data probably show a temporal increasing trend. Since the salinity data seem to drift, it is expected, that the estimated vertical diffusion coefficient K_S, based on the observed rate of change of salinity, is not reliable. As shown in the chapter below (3.4.1.), this increasing trend is caused by drifting of the conductivity sensor and with an appropriate calibration it was possible to be removed.

After the estimations of the temporal and vertical gradient, according to the equation (6) (in chapter2.5.), the actual estimation of the eddy diffusivity coefficient was possible:

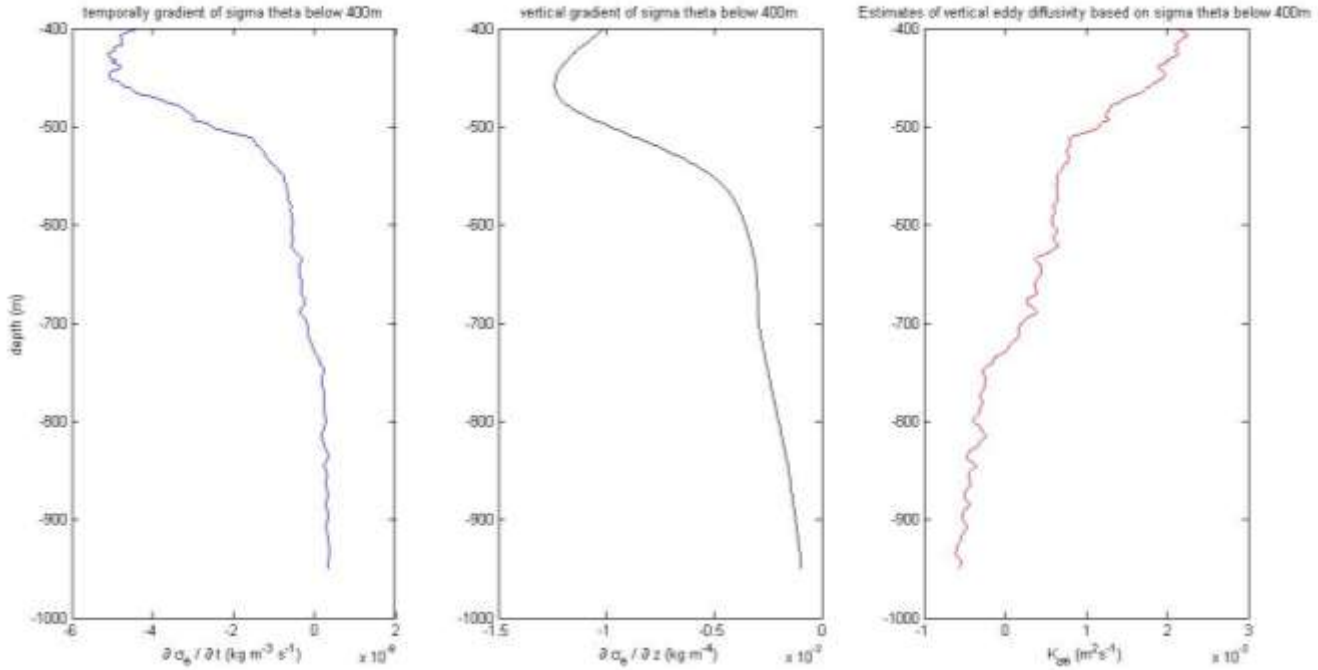

Figure 24.) The temporal (left) and the vertical (middle) gradient of σ_θ and the estimation of the vertical eddy coefficient $K\sigma_\theta$ (right)

The final graph of the vertical eddy diffusion coefficient $K_{\sigma\theta}$, K_S, K_T, based on all three parameters is represented below in a logarithmic scale:

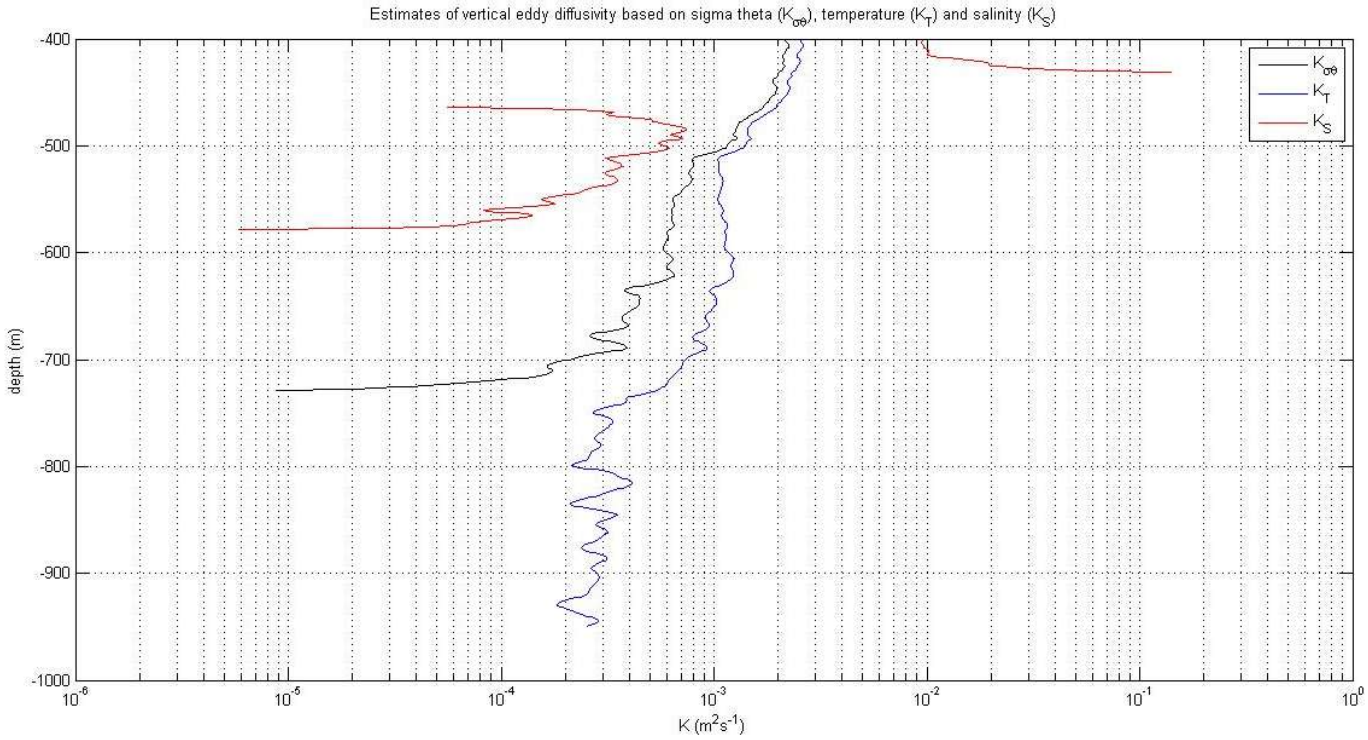

Fig.25.) Estimates of vertical eddy diffusivity based on salinity (K_S:red line), temperature (K_T:blue line) and density ($K_{\sigma\theta}$: black line)

As it can be seen in the figure above, the vertical eddy diffusion coefficient K_c (z) was found to range between 10^{-5} - 10^{-3} m^2s^{-1} between 400 and 1000 m below the surface (Fig.25.) . As it was expected after the Θ/S graph, the coefficient K_S indicates some uncharacteristic salinity measurements, which might be caused by drifting of the conductivity sensor. It can be suggested, that the other two eddy coefficients ($K_{\sigma\theta}$ and K_T) represent a good agreement in the first 100-200m. Furthermore, with an appropriate calibration it could be possible that all the three coefficients would show agreement, suggesting that the dominant process in vertical diffusion is turbulent mixing.

3.4.1.) Correction of vertical diffusion by calibrating conductivity

In order to prove the existence of the conductivity sensor drift, it was examined if the temperature at the θ/S diagram, for deeper than 400m waters, keeps related to the same salinity during the stagnation period. More specific, for a chosen depth of 820 meters (D_{fit}) the conductivity on the same isotherm was calculated, considering that the salinity is expected to remain constant at a constant temperature. In order to determine the rate of the conductivity and to apply it on the data set, the measured *In-situ* conductivity ($C_{in\text{-}situ}$:from raw float) and the calculated one (C_{fit}: corresponding to the initial salinity, but at the right temperature) were estimated at the chosen depth (D_{fit}). With the conductivity correction it was possible to calculate the corrected salinity and density values once again as well as to estimate the correct vertical eddy diffusion coefficient.

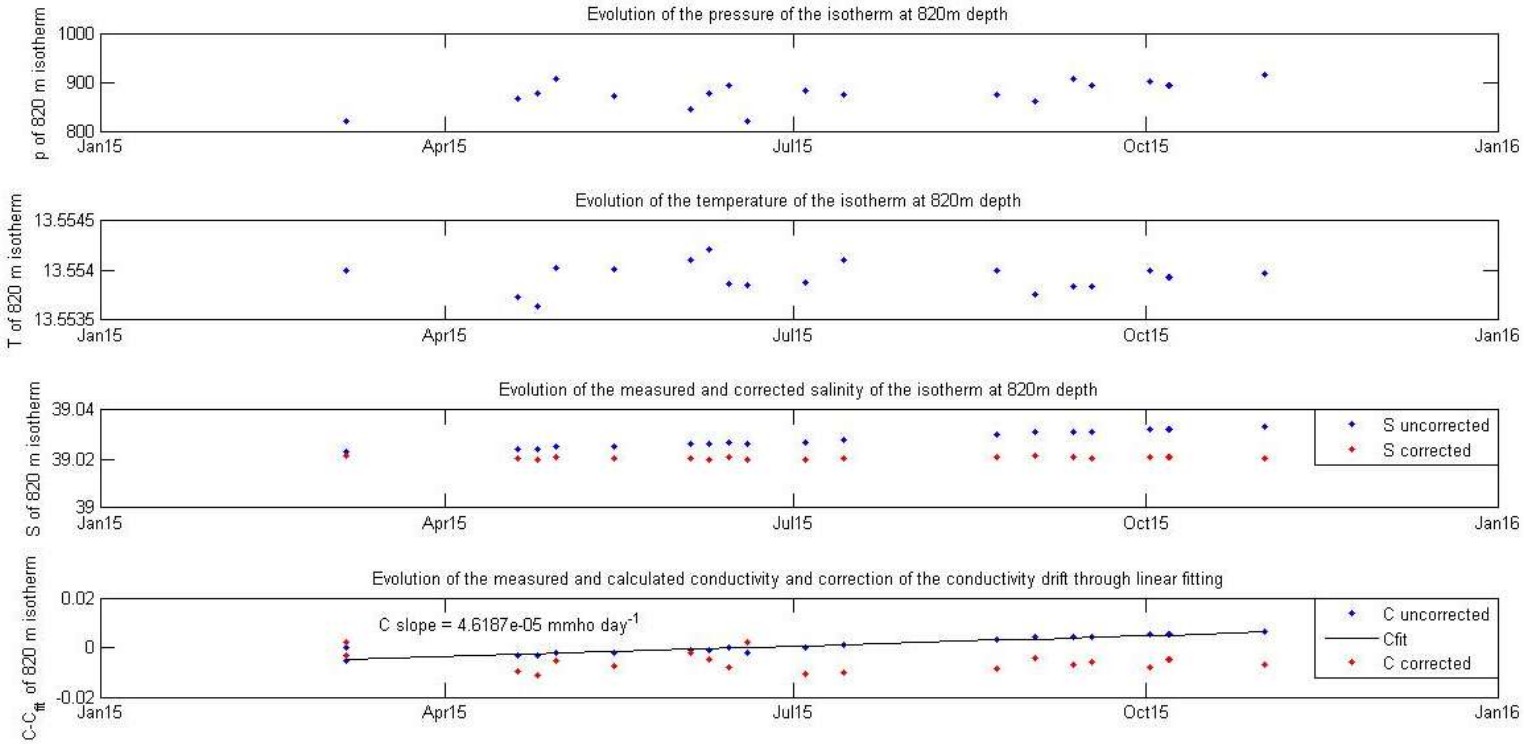

Fig.26.) Estimation of the conductivity drift based on the calculation of the slope between the raw and the corrected conductivity values

As it appears in the figure above (Fig.26.), the salinity seems indeed to drift towards higher values, due to the fact that the conductivity sensor presents increasingly higher values than expected. After the linear fitting, with the correction slope being equal to $4{,}6187\times10^{-5}$ mmho day^{-1}, the properties of the deeper than 400m water masses during the stagnation period seem to slide clearly along the θ-S curve towards lower densities:

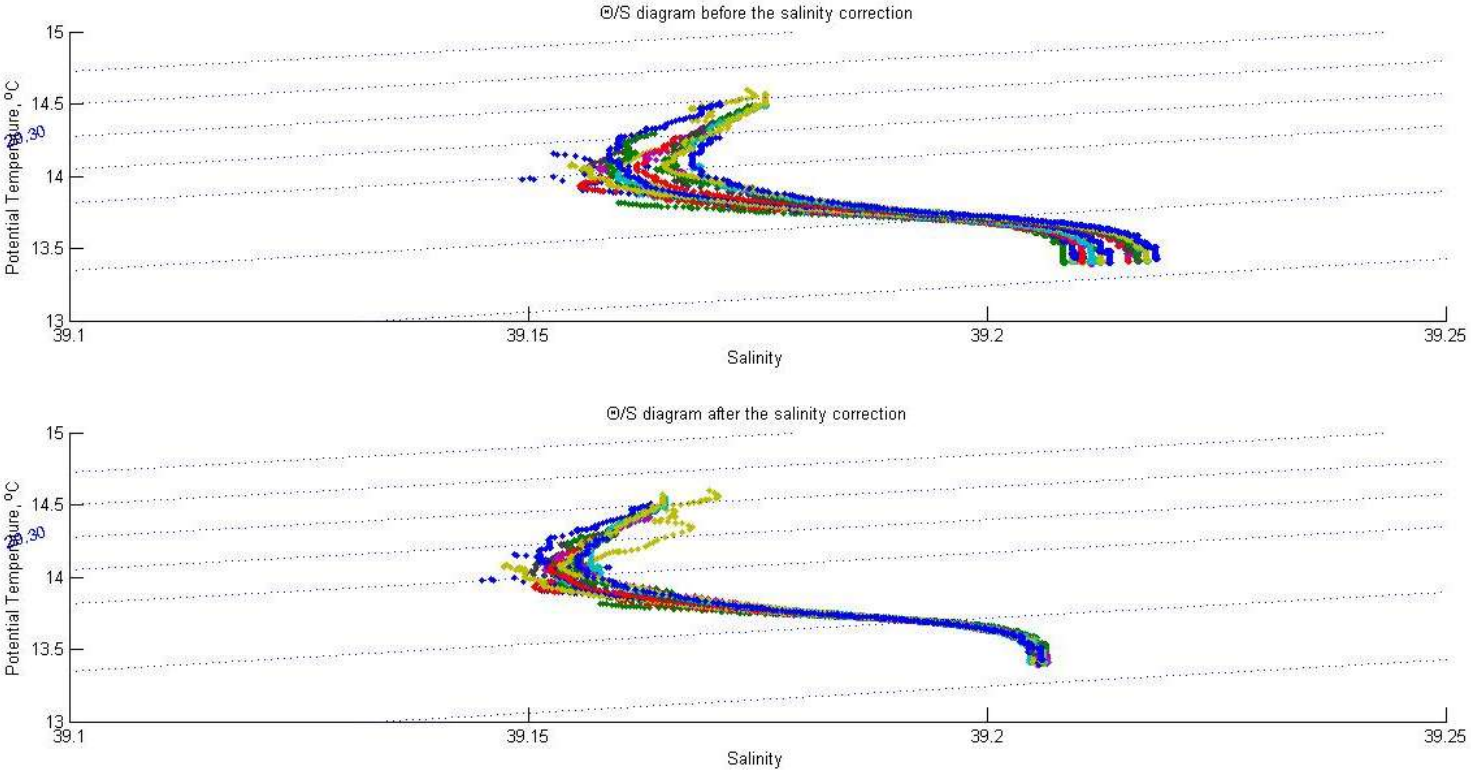

Fig.27.) Θ/S diagram before and after the salinity correction

The improvement and importance of the conductivity sensor calibration can be noticed in the diagrams above. The corrected values seem to lie along the same curve and the temporal increasing trend is eliminated. A good agreement of all the vertical eddy coefficients K_c might improve that the dominant process in vertical diffusion is probably turbulent mixing. The estimates of vertical eddy diffusivity before and after the conductivity sensor calibration in the figures are represented below (Fig.28.)

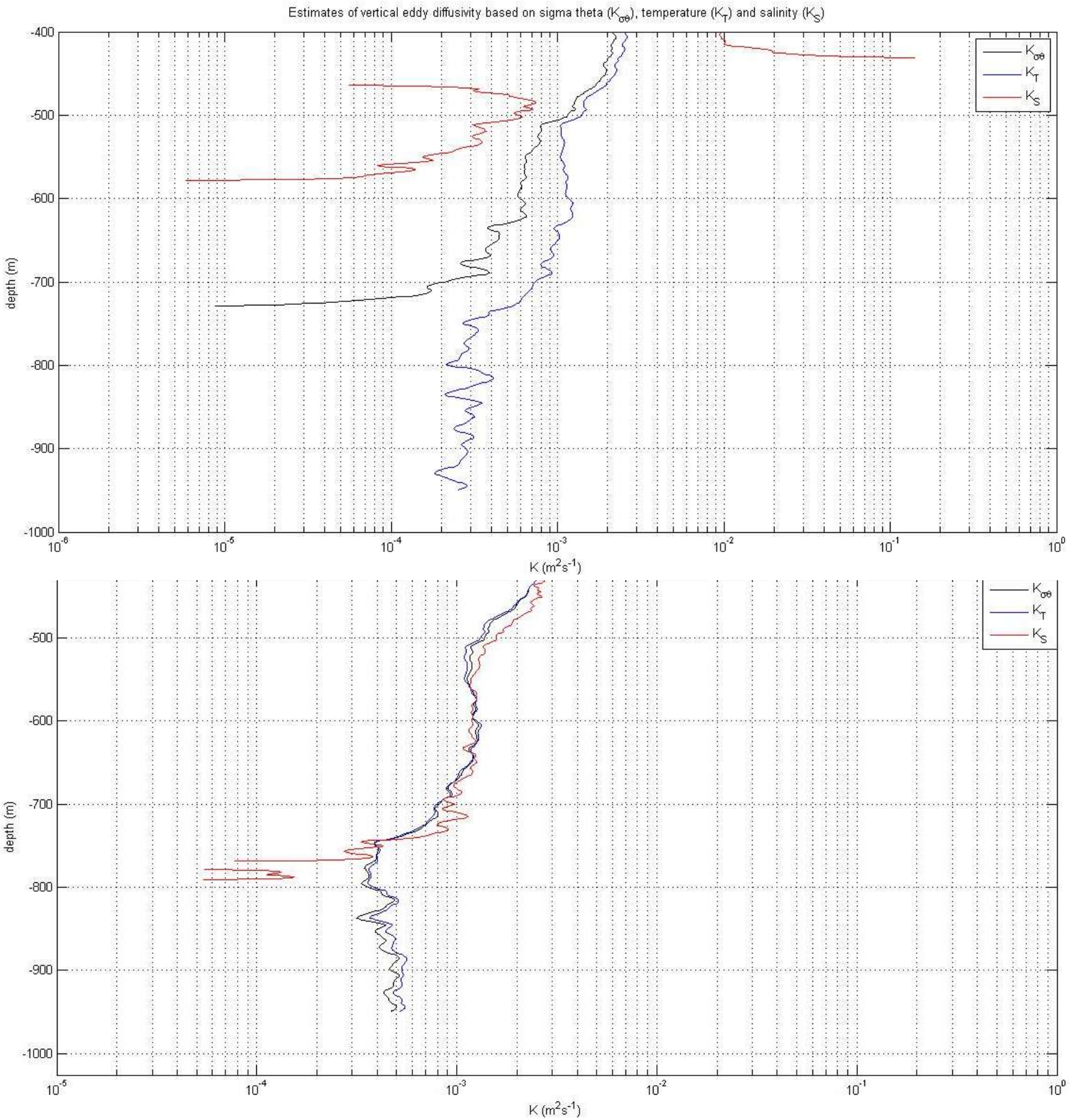

Fig.28.) Estimates of vertical eddy diffusivity based on salinity (K_S:red line), temperature (K_T:blue line) and density ($K_{\sigma\theta}$: black line) before (above) and after (below) the conductivity sensor calibration

The results of the calibration demonstrate, that the MedArgo float sensor nr. 6901884 exhibited a remarkable positive drift in salinity of 0,0039 to 0,0112 psu due to the conductivity sensor drift. This indicates that the drift increases to the operating period of the float. The increasing rate of conductivity is $4{,}6748\times10^{-5}$ mmhoday^{-1}, which yields a drift of 0,0105 mmho throughout the stagnation period. After the necessary corrections, the three vertical eddy coefficients K_c were found to range between $6\text{-}7\times10^{-5}$ and $2\text{-}3\times10^{-3}$ m^{2}s^{-1} for the deeper than 400m waters. It is noteworthy, that the coefficients show an improved agreement after the sensor calibration. Especially until the depth of 700m all three of them seem to extend between 7×10^{-4} and 3×10^{-3}m^{2}s^{-1}, indicating that the dominant process in vertical diffusion was possibly turbulent mixing. In order to assess these estimates, they were compared with the estimations (~10^{-4} m^{2}s^{-1}) of Zervakis et al. (2003). The comparison suggests that the estimates values are most likely to be realistic.

4.) Conclusion and Discussion

The analyzed vertical and seasonal hydrographic characteristics indicate that the Black Sea Water surface layer is an effective isolator between the deep layers of the North Aegean and the atmosphere. It seems that dense water formation events demand not only large exchange of buoyancy with the atmosphere, but also a significant reduction of the water surplus of the Black Sea. This combination of necessary factors for deep water formation in the North Aegean probably reduces the frequency of such events. Between those events, the bottom waters are excluded from interaction with other water masses through advection and they progressively change slowly, relaxing towards a less dense and more homogeneous state through vertical turbulent diffusion. It should be mentioned that the specific calculations may overestimate the vertical eddy diffusivity coefficients due to isopycnal mixing as projected on the vertical direction. The estimated diffusivities fall well within the similarly estimated values of Zervakis et al. (2003), which however represented longer time-scales. Also large values of K_C should be expected, considering the small size of the North Aegean sub-basins as well as the proximity to the continental slope.

It is noteworthy that it was possible to examine the behavior of the basin at shorter-than-annual time scales, due to the fact that the ARGO profiling float was trapped within the deep Athos basin. This opportunity also made it possible for the first time to calibrate the conductivity sensor of the specific NOVA-type float based on new, high-frequency data from the deep layers during a stagnation period. The sensor drift correction method widely used by the Argo community (e.g. Davis et al., 2001; Böhme and Send, 2005; Owens and Wong, 2009; Wang et al., 2013), is the method by Wong et al. (2003). According to this method, float data are checked in an indirect way, such as comparisons with climatology or shipboard high-resolution CTDs. In most cases they revealed much smaller negative drifts of the profiling floats due to bio-fouling and cell contamination. Positive drifts, as the one exhibited in this thesis, are still not well understood. A comparison between different methods will be the next step to do in order to evaluate this calibration.

Furthermore, it might be of oceanographic interest to examine the long-term hydrographic variability of the deep waters based on high-frequency data. A future dedicated experiment with either an intentionally trapped profiling float, or using profiling moored instruments, would provide important information about the behavior of deep basins in the North Aegean.

5.) References

Androulidakis, Y., Kourafalou, V., Krestenitis, Y., Zervakis, V., 2012. Variability of deep water mass characteristics in the North Aegean Sea: the role of lateral inputs and atmospheric conditions. *Deep Res Part I Oceanogr Res Pap* 67, 55–72.

Balopoulos, E., Theocharis, A., Kontoyiannis, H. , Varnavas, S., Voutsinou-Taliadouri, F., Iona, A., Souvermezoglou, A., Ignatiades, L., Gotsis-Skretas, O., Pavlidou, A., 1999). Major advances in the oceanography of the southern Aegean Sea-Cretan Straits system (eastern Mediterranean*), Prog. Oceanogr., 44,* 09–130.

Böhme, L., Send, U., 2005. Objective analyses of hydrographic data for referencing profiling float salinities in highly variable environments. *Deep-Sea Research II* 52, 651–664.

Georgiou, S., Mantziafoua, A., Sofianos, S., Gertmanb, E., Özsoyc, S., Somot, V., Vervatisa, V., 2014. Climate variability and deep water mass characteristics in the Aegean Sea.

Georgopoulos, D., Salusti, E., Theocharis, A., 1992. Deep water formation in the N. Aegean Sea. *Ocean Modelling*, 95, 4-6.

Georgopoulos, D., Theocharis, A., Zodiatis, G., 1989. Intermediate water formation in the Cretan Sea (South Aegean Sea). *Oceanologica Acta*, 12 (4), 353-359.

Davis, R., Sherman, J., Dufour, J., 2001. Profiling ALACEs and other advances in autonomous subsurface floats. *J. Atmos. Ocean. Technol.* 18, 982–993.

de Boyer Montégut, C., Madec, A., Fischer, S., Lazar, A., Iudicone, D., 2007. Mixed layer depth over the global ocean: An examination of profile data and a profile-based climatology*, J. Geophys. Res., 109.*

IOC, SCOR, IAPSO, 2010. The international thermodynamic equation of seawater – 2010: Calculation and use of thermodynamic properties. *Intergovernmental Oceanographic Commission, Manuals and Guides No. 56, UNESCO*,196.

Lykousis, V., et al. (2002), Major outputs of the recent multidisciplinary biogeochemical researches undertaken in the *Aegean Sea, J. Mar. Syst., 33–34,* 313–334.

Nielsen, J., 1912. Hydrography of the Mediterranean and adjacent waters, *in Report of the Danish Oceanographic Expedition 1908–1910 to the Mediterranean and Adjacent Waters, vol. 1,* 72–191.

Nittis, K., Lascaratos, A., Theocharis, A., 2003. Dense water formation in the Aegean Sea: numerical simulations during the Eastern Mediterranean Transient. *Journal of Geophysical Research 108*, 8120.

Owens, W., Wong, A., 2009. An improved calibration method for the drift of the conductivity sensor on Autonomous CTD profiling floats by θ-S climatology. *Deep-Sea Research Part I* 56 (3), 450–457.

Papadopoulos, V., Bartzokas, A., Chronis, T., Georgopoulos, D., Ferentinos, G., 2012. Factors regulating the air-sea heat fluxes in the Aegean Sea, *J. Clim., 25,* 491–508.

Plakhin, Y., 1972. Vertical winter circulation in the Mediterranean, *Oceanology, Engl. Transl., 12,* 344–351.

Poulos, S., Drakopoulos, P., Collins, M., 1997. Seasonal variability in sea surface oceanographic conditions in the Aegean Sea (eastern Mediterranean): *An overview, J. Mar. Syst.,* 13, 225–244.

Theocharis, A., Georgopoulos, D., 1993. Dense water formation over the Samothraki and Lemnos plateaus in the north Aegean Sea (eastern Mediterranean Sea), *Cont. Shelf Res.,* 13, 919–939.

Tragou, E., Zervakis, V., Papadopoulos, A., Maderich, V., Georgopoulos, D., Theocharis, A.,2003. Buoyancy transport through the Aegean Sea, in 2nd International Conference on Oceanography of the Eastern Mediterranean and Black Sea: Similarities and Differences of Two Interconnected Basins, edited by Yilmaz, A., 38–46*, Tübitak Publi.,* Ankara.

Ünlüata, U., Oğuz, T., Latif, M., Ozsoy, E., 1990. On the physical oceanography of the Turkish Straits. *The Physical Oceanography of Sea Straits,* L. J. Pratt (Ed.), Kluwer Academic Publishers, 25-60.

Velaoras, D., Lascaratos, A., 2005. Deep water mass characteristics and interannual variability in the North and Central Aegean Sea. *Journal of Marine Systems, 53*, 59-85.

Velaoras, D., Lascaratos, A., 2010. North-Central Aegean Sea surface and intermediate water masses and their role in triggering the Eastern Mediterranean Transient. *Journal of Marine Systems, 83*, 58-66.

Vervatis, V., Sofianos, S., Theocharis, A., 2011. Distribution of the thermohaline characteristics in the Aegean Sea related to water mass formation processes (2005-2006 winter surveys). J*ournal of Geophysical Research*, (116), C09034.

Wong, A.,J ohnson, G., Owens,W., 2003. Delayed-mode calibration of autonomous CTD profiling float salinity data by θ–S climatology. *Journal of Atmospheric and Oceanic Technology* 20, 308–318.

Wüst, G., 1961. On the vertical circulation of the Mediterranean Sea. *Journal of Geophysical Research, 66 (10)*, 3261-3271.

Yu, L., Jin, X., 2011. Satellite-based global ocean vector wind analysis by the Objectively Analyzed Air-sea Fluxes (OAFlux) Project: Establishing consistent vector wind time series from July 1987 onward through synergizing microwave radiometers and scatterometers.

Yu, L.,Weller, R., 2007. Objectively Analyzed air-sea heat Fluxes (OAFlux) for the global ocean, Bull. *Am. Meteorol. Soc., 88(4*), 527–539.

Zervakis, V. and Georgopoulos, D., 2002. Hydrology and circulation in the North Aegean (eastern Mediterranean) throughout 1997 and 1998.

Zervakis, V., Georgopoulos, D., Drakopoulos, P., 2000. The role of the North Aegean in trigerring the recent Eastern Mediterranean climatic changes. *Journal of Geophysical Research C: Oceans*, 105 (C11), 26103-26116.

Zervakis, V., Georgopoulos, D., Karageorgis, A., Theocharis, A., 2004. On the response of the Aegean Sea to climatic variability: a review. *Int. J. Climatol. 24*, 1845–1858.

Zervakis, V., Krasakopoulou, E., Georgopoulos, D. & Souvermezoglou, E., 2003. Vertical diffusion and oxygen consumption during stagnation periods in the deep North Aegean. *Deep-Sea Research I*, 50, 53-71.

Zervakis, V., Krasakopoulou, E.,Tragou, E.,Kontoyiannis, H.,Kioroglou, S., 2009.Interannual variability of the deep layers in the North Aegean. *Proceedings of the 9th Helllenic Symposium of Oceanography and Fisheries.* Vol 1. Patras, Greece, 462–467.

Zervakis, V., Theocharis, A., Georgopoulos, D., 2005. Circulation and hydrography of the open seas, 104-110. In: *State of the Hellenic Marine Environment*. Papathanasiou, E. & Zenetos, A. (Eds) HCMR, Athens.

Zodiatis, G.,1994. Advection of Black Sea water in the north Aegean Sea, Global Atmos. *Ocean Syst., 2,* 41–60.